https://doi.org/10.5194/amt-2019-316
Preprint. Discussion started: 23 October 2019

Atmospheric Measurement Techniques Discussions

Impact of isotope composition on the humidity dependency correction of water vapour isotope measurements with infra-red cavity ring-down spectrometers

Yongbiao Weng[1,2], Alexandra Touzeau[1,2], and Harald Sodemann[1,2]

[1]Geophysical Institute, University of Bergen, Bergen, Norway
[2]Bjerknes Centre for Climate Research, Bergen, Norway

Correspondence to: Yongbiao Weng (yongbiao.weng@uib.no)

Abstract.

Advances in laser spectroscopic techniques now enable high-frequency in situ measurements of the water vapour isotope composition on platforms such as ship and aircraft. However, the isotope compositions and the *d*-excess measured by this technique can be substantially affected by water concentrations, especially at low humidity. This measurement artefact is known as the "humidity dependency", and is commonly corrected for uniformly across all isotope compositions. Here we systematically investigate the behaviour of the humidity dependency on three commercial cavity ring-down spectrometers for different water standards within a humidity range of 500 to 23'000 ppmv. We find that the isotope compositions of measured water do have a substantial impact on the shape of the humidity dependency at low humidity (below 4'000 ppmv). This isotope composition dependency can, for example, create an offset of ± 0.5 and ± 6 ‰ for δ^{18}O and δD at $\sim$2'000 ppmv in the case of a Picarro L2130-i, resulting in an offset of 2–3 ‰ for the *d*-excess. We show that the combined isotope composition–humidity dependency can be expressed by a surface function, which allows to build a correction framework. The impact of this correction is illustrated for a case of aircraft measurements and ship-based measurements in cold environments. A systematic assessment of the robustness of our findings for three laser spectrometers shows overall constant behaviour with time (for periods ranging from one month to two years), independent of the method of characterisation (discrete liquid injection and continuous vapour streaming), dry gas supply (N_2 and synthetic air), or the sequence of humidity levels. Based on our analysis, we recommend a procedure for the characterisation and subsequent correction of the combined isotope composition–humidity dependency for this type of laser spectrometers when performing water vapour measurements in cold and dry conditions.

1 Introduction

Stable water isotopes (hydrogen and oxygen) are natural tracers in the atmosphere and hydrosphere, and have long been used to improve our understanding of the hydrological cycle and climate processes (Dansgaard, 1953, 1954; Gat, 1996). Advances in laser spectroscopic techniques now allow high-frequency in situ measurements of isotope compositions of water vapour in the atmosphere (Kerstel, 2004; Kerstel and Gianfrani, 2008). One commercially available instrument of this type is the Cavity Ring-Down Spectrometer (CRDS) manufactured by Picarro Inc., USA. The measurement principle of CRDS is based upon

https://doi.org/10.5194/amt-2019-316
Preprint. Discussion started: 23 October 2019

Atmospheric Measurement Techniques Discussions

the absorption of a laser pulse at a wavelength specific to a given isotopologue (Crosson, 2008). The CRDS has an optimal performance within a humidity range of 19'000∼21'000 ppmv, where signal-to-noise ratios enable precise measurements. Beyond this optimal humidity range, the measurement uncertainty increases. Additionally, the measurement suffers from a bias depending on the humidity level. While liquid measurements are performed within the optimal humidity range, in situ water vapour measurements in the atmosphere are commonly not constrained to this optimal humidity range. The fact that the humidity in the atmosphere can vary from below 500 ppmv in cold and dry regions (e.g., polar regions or the middle and upper troposphere) to about 30'000 ppmv in warm and humid regions (e.g., tropics) requires an appropriate correction to this *humidity dependency* for high-quality in situ measurements of atmospheric water vapour.

Humidity dependency, sometimes named concentration dependency (Wen et al., 2012; Bailey et al., 2015) or water vapour mixing ratio dependency (Aemisegger et al., 2012) of infra-red laser spectrometers for water isotopes is a prominent source of measurement bias and has been described in numerous studies (e.g., Lis et al., 2008; Schmidt et al., 2010; Sturm and Knohl, 2010; Steen-Larsen et al., 2013, 2014; Bastrikov et al., 2014). Many studies found the humidity dependency to be nonlinear and to some extent specific to both the instrument used and the isotope composition measured. For example, reviewing the then available characterisation systems on a Picarro L1115-i and L1102-i, Wen et al. (2012) showed that the humidity dependency could vary for each specific instrument. Aemisegger et al. (2012) demonstrated that the humidity dependency is different for different instrument types and generations, and found that a dry gas supply of dried ambient air using a dry unit (Drierite) or synthetic dry air from a gas cylinder can affect the humidity dependence behaviour. However, they did not find a substantial impact of the isotope composition after testing four different standards. Bonne et al. (2014) suspect the different humidity dependency functions at low humidity levels (below 2'000 ppmv) for their two working standards to be likely artefact of residual humidity in the dry air dried by Drierite. Bailey et al. (2015) shows that the humidity dependence is clearly different for the tested three standard waters, while emphasizing the uncertainty from statistical fitting where the characterisation data are infrequent. Sodemann et al. (2017) found a substantial impact of the humidity dependency correction when processing aircraft measurements of d-excess over the Mediterranean, but did not account in detail for different isotopic standards. Bonne et al. (2019) has characterised the humidity dependency of their isotope measurements throughout the Atlantic and Arctic Oceans using four water standards. They did not observe any significant drift for measurements separated by several months. However, they found that the humidity dependency does depend on the isotopic standard used.

To summarize, in these previous studies, the impact of the isotope composition of measured standards on humidity dependence has not been recognized as a significant bias source, or has so far not been systematically investigated, in particular for very low humidities. We hypothesize that a potential isotope composition dependence could have been masked by the different versions of the laser spectrometers and the different characterisation methods (e.g., characterisation system, dry gas supply, etc.) used in these studies.

Here we carry out a systematic analysis on the humidity dependence behaviour of three CRDS analysers, one Picarro L2130-i and two Picarro L2140-i. Using five standard waters with different isotope compositions, we characterise the impact of isotope composition of the standard water on the humidity dependence behaviour for each analyser. Based on the characterised isotope composition–humidity dependence, a correction scheme is developed. We then identify the robustness of the isotope

https://doi.org/10.5194/amt-2019-316
Preprint. Discussion started: 23 October 2019

Atmospheric Measurement Techniques Discussions

composition–humidity dependence across three analysers, two characterisation methods, two dry gas supplies, two measuring sequences, and with respect to time at monthly to yearly time scales. Finally, we demonstrate the impact of the humidity dependence correction on the vapour measurement during a cold air outbreak event and an aircraft campaign, and provide recommendations on how to apply the correction scheme to other analysers.

2 Methods and data

Because of the large impact of the correction on a range of measurement at the low humidity where instrument noise is high, in this section we carefully test the validity across a range of possible influencing factors, thereby excluding possible artefacts. These influencing factors include the method to generate the vapour, the specific analyser that is used, the potential instrument drift over time, the possible artefacts introduced by the matrix gas and the measuring sequence of the humidity steps. We have therefore designed in total 14 experiments (Table 2) to evaluate all these factors separately and repeatedly. These 14 experiments can be separated into five categories with respect to their aims (Table 3). With these five categories, we assess the dependence on vapour generating method, the dependence on the tested instrument, the long term stability of the dependence behaviour, the influence from dry gas supply and the influence from the measuring sequence. In the end, we introduce the in situ measurement data that are used to illustrate the impact of correction.

2.1 Quantification of the isotope composition and $\Delta\delta$ notation

The abundance of stable water isotopes in a reservoir is quantified by isotope ratios, defined as the ratio of concentrations of the heavy, rare isotopologue ($HD^{16}O$ or $H_2^{18}O$) to the abundant, light isotopologue ($H_2^{16}O$). For example, the isotope ratio of hydrogen in a water reservoir is:

$$^2R = \frac{[HD^{16}O]}{[H_2^{16}O]}. \tag{1}$$

The absolute value of R is very small (typically consisting of 5–6 digits). In addition, the absolute ratios are in principle less relevant than the changes in ratios occurring during phase transitions. Therefore, an isotope abundance is generally reported as a deviation of the isotope ratio of a sample relative to that of a standard, known as δ notation:

$$\delta = \frac{R_{\text{sample}} - R_{\text{standard}}}{R_{\text{standard}}} \cdot 1000\,‰. \tag{2}$$

A δ value for water isotopes is generally indicated in per mil (‰) relative to the internationally accepted Vienna Standard Mean Ocean Water (VSMOW2), distributed by the International Atomic Energy Agency (IAEA) at Vienna (IAEA, 2009); it is directly used to represent the isotope composition of the water sample.

The magnitude of the bias introduced by the humidity dependence appears to be at least one order smaller than the span of the isotope compositions of the measured standards. To focus on the bias dependency on humidity, we introduce here the $\Delta\delta$ notation, defined as the deviation of the measured isotope compositions at various humidities (δ_{meas}) from the isotope

https://doi.org/10.5194/amt-2019-316
Preprint. Discussion started: 23 October 2019


Atmospheric Measurement Techniques Discussions

composition at a reference humidity (δ_{ref}):

$$\Delta\delta = \delta_{\text{meas}} - \delta_{\text{ref}}. \tag{3}$$

The reference humidity is chosen to be 20'000 ppmv where the CRDS provides optimal performance. The isotope composition at 20'000 ppmv is obtained by a linear interpolation between the closest measurements above and below 20'000 ppmv (mostly between 19'000 and 21'000 ppmv). Note that all the presented humidities in this study are raw measurements from the CRDS, since the humidity dependency correction is applied to raw data before calibration.

While $\Delta\delta^{18}$O and $\Delta\delta$D are given directly by the definition above, Δd-excess is a secondary parameter that is obtained from calculation: firstly we calculate d-excess at each data point from corresponding δ^{18}O and δD with the definition $d\text{-excess} = \delta\text{D} - 8 \cdot \delta^{18}\text{O}$ (Dansgaard, 1964); then we obtain Δd-excess by calculating the deviation of the d-excess at each data point from the d-excess at the reference humidity (20'000 ppmv). The obtained $\Delta\delta^{18}$O, $\Delta\delta$D and Δd-excess are used to determine isotope composition–humidity dependency functions in Sect. 3 and Sect. 4.

2.2 Characterisation methods

We have used two methods to characterise humidity dependence behaviour of the three instruments: discrete liquid injections and continuous vapour streaming. These are essentially two ways of generating a vapour sample to be analysed by the spectrometer. Both methods require injection of a liquid standard water into a heated evaporation chamber where the injected water is completely evaporated and mixed with a dry carrier gas. The former method generates a fixed amount of vapour sample by a single injection from a syringe, while the latter one continuously delivers liquid water from a syringe pump, and generates a continuous vapour stream lasting in practice 20–30 min.

2.2.1 Discrete liquid injections

Standard water is injected from 1.5 ml PTFE/rubber-septum sealed vials with a 10 μl syringe (VWR, Part No.: 002977). Injections are operated by an autosampler (A0325, Picarro Inc, USA) or by manual injection. Vaporization of liquid water is achieved within a Picarro vaporizer (A0211, Picarro Inc, USA) set to 110 °C. The vaporizer then obtains synthetic air (synthetic air 5.5, purity 99.9995%, Praxair Norge AS) or N_2 (Nitrogen 5.0, purity > 99.999%, Praxair Norge AS) from a gas cylinder at a pressure set to ∼2.5 psi. The vaporizer chamber seals off for a few seconds to allow sufficient mixing between vapour and dry air, before delivering the mixture to the analyser at a highly stable humidity level.

Each time before switching to a new standard water, 8–12 injections of the new standard water at a humidity level of ∼20'000 ppmv were applied to account for memory effects from the previous injections. Then the sequence begins from the lowest (∼500 ppmv) and ends to the highest (∼ 23'000 ppm) humidity level. Various humidity levels are obtained by adjusting the injection volume in the 10 μl syringe. Injection volume was modified to be between 0.05 and 2.5 μl with a step of 0.05 μl, resulting in humidity levels between approximately 500 and 23'000 ppmv with a step of ∼450 ppmv. Four injections in high precision mode (longer measurement period, approximate 10 min per injection) were applied at each humidity level, and the last three injections were then averaged for further analysis. Injections with an injection volume of 2 μl (∼19'000 ppmv) were

https://doi.org/10.5194/amt-2019-316
Preprint. Discussion started: 23 October 2019


Atmospheric Measurement Techniques Discussions

carried out at the beginning and end of a sequence to account for potential instrument drift. A sequence for one standard water approximately lasts 35 hours. The instrument drift within a sequence has typically a magnitude of 0.05±0.02‰, 0.7±0.1 ‰ and 0.4±0.1 ‰ for δ^{18}O, δD and d-excess, respectively. The drift is 3–7 times larger than the measurement uncertainty but one order smaller than the bias introduced by the humidity dependence; it is corrected by assuming a temporal linearity during the sequence period.

Manual liquid injections were carried out during a field deployment where no autosampler was available. During manual injections, it is challenging to maintain a constant injection volume, and thus difficult to achieve precise humidity levels. In this case, only injection volumes between 0.2 and 1.6 μl with a step of ∼0.2 μl are employed (roughly corresponding to humidity levels between 2'400 and 24'000 ppmv with a step of ∼3'000 ppmv). With fewer steps, a sequence for one standard water with manual injection only lasts about 6 hours. Despite the shorter measurement period, the instrument drift within a sequence increased by a factor of 2–3 for δ^{18}O and δD, being 0.16±0.03 ‰ and 1.65±0.18 ‰ respectively, resulting in a drift of 0.37±0.22 ‰ for d-excess. The relatively high instrument drift compared to the autosampler injections in the laboratory is most likely due to the uncertainty introduced by the inconstant injection volume and the installation on a mobile platform (a research vessel in our case). The drift is again corrected by assuming a temporal linearity during the sequence period.

2.2.2 Continuous vapour streaming

A continuous vapour stream is generated via a so-called standard delivery module (SDM, A0101, Picarro Inc, USA). The SDM is a device with two syringe pumps, that provides automated delivery of two standard waters at up to three water concentrations per standard. The standard water is delivered to the Picarro vaporizer, where the standard water is instantly vaporized at 140 °C and simutaneously mixed with dry gas. Various humidity levels between 600 ppmv and 24'000 ppmv were obtained by adjusting liquid water injection speed of the syringe pumps from 0.002 $\mu l\, s^{-1}$ to 0.8 $\mu l\, s^{-1}$. The generated standard vapour is continuously delivered to and measured by the spectrometer. During the characterisation, a total of about 25 humidity levels with an humidity step of ∼1'000 ppmv (0.003$\mu l\, s^{-1}$) have been measured for each standard water. Each humidity level is measured for 20–40 minutes and the averaged value of a 5 minutes period close to the end of the measurement is used in the analysis. Due to unstable calibration performance, only 1–2 min long sections were used for the characterisations done in July 2016 and Feb 2018 for the standard DI on instrument HIDS2254.

A measurement sequence of standard GSM1 with ambient air dried through Drierite shows that the magnitude of the instrument drift during a 22 hour measurement with SDM is similar to that of the liquid injection with an autosampler. However, due to the lower precision with SDM measurement, the instrument drift is comparable (0.10±0.09 ‰ and 0.96±0.36 ‰ for δ^{18}O and δD respectively) or smaller (0.24±0.78 ‰ for d-excess) compared to the measurement uncertainty. Therefore, except for the measurement with standard GSM1 above, the measurements with SDM are not corrected for instrument drift.

2.3 Instruments

The instruments investigated in this study include two Picarro L2140-i (serial numbers HKDS2038 and HKDS2039) and one Picarro L2130-i (serial number HIDS2254), the latter being custom-modified with an option for higher data acquisition

https://doi.org/10.5194/amt-2019-316
Preprint. Discussion started: 23 October 2019


Atmospheric Measurement Techniques Discussions

and flow rate. Hereafter, we refer to each instrument with the corresponding serial number. To convert observed absorption intensity to actual water concentration and to minimize instrument drift, these CRDS systems precisely control the pressure and temperature of their cavities to be at 80°C and 50 Torr. The typical measurement range for vapour is 1'000 to 50'000 ppmv (certified down to 200 ppmv for the instrument HIDS2254). During the experiments, all instruments were running in low flow mode with a sample inlet flow rate of ∼35 sccm and a measurement frequency of ∼1.25 Hz.

2.4 Standard waters

To identify the dependency on the isotope composition, we have applied multiple internal standard waters to characterise the humidity dependence. The standard waters include four laboratory standards in use at Facility for Advanced Isotopic Research and Monitoring of Weather, Climate and Biogeochemical Cycling (FARLAB), University of Bergen and three laboratory standards in use at the Isotope Laboratory of University of Iceland (UI) (Table 1). For the FARLAB standards, one is obtained from snow in Greenland (GSM1), one made of mountain snow from Norway (VATS), one that consists of deionized tap water at Bergen (DI), one made of evaporated DI water (EVAP). Besides the four laboratory standards, we have also used an even mixing between GSM1 and VATS (named MIX) and the uncalibrated deionized tap water (DI (tap)). For the UI standards, one is from snow at NEEM ice core drilling site in Greenland (NEEM), one consists of groundwater in Reykjavik (GV) and one made of Milli-Q purified water based on ocean water from Bermuda (BERM). The isotope compositions of all the used waters span from -33.52 to 5.03 ‰ and from -262.95 to 6.26 ‰ for δ^{18}O and δD respectively (Table 1).

For the measurement using discrete liquid injection, we applied 3–5 FARLAB standard waters with an autosampler and three UI standard waters with manual injections. As the continuous vapour streaming is primarily used for testing the robustness of humidity dependence, we only applied the standards GSM1 and DI with this vapour generation method.

2.5 Dry gas supply

The type of dry gas supply may have an influence on the characterisation of humidity dependence (Aemisegger et al., 2012). The manufacturer recommends a customer-supplied gas drying unit (e.g. Drierite desiccants) to supply dry gas for the SDM unit. However, the ambient air dried through Drierite can still contain a certain amount of moisture (typically below 200 ppmv when the ambient humidity is around 10'000 ppmv), which can contribute to the measured isotope ratio at low humidity levels (e.g., 10% below 2'000 ppmv). In most of our experiments we have replaced the gas drying unit to dry gas cylinders that contain synthetic air (synthetic air 5.5, purity 99.9995%, Praxair Norge AS) or N_2 (Nitrogen 5.0, purity > 99.999%, Praxair Norge AS). We have tested all the three types of dry gas supply with the characterisation on instrument HIDS2254 for continuous vapour streaming. We also carried out the test of synthetic air and N_2 for discrete liquid injections.

https://doi.org/10.5194/amt-2019-316
Preprint. Discussion started: 23 October 2019

Atmospheric Measurement Techniques Discussions

2.6 In situ measurement data for studying the impact of isotope composition–humidity dependency correction

To demonstrate the impact of the isotope composition–humidity dependence correction on the measurement, we applied the correction scheme to two datasets obtained from in situ vapour measurements during the Iceland Greenland Seas Project in March 2018 onboard an aircraft and a research vessel respectively (Renfrew et al., 2019).

The analyser HIDS2254 was employed for the measurement onboard the aircraft. The instrument was fixed on a rack on the left side of the non-pressurized cabin of a Twin Otter aircraft. A metal tube with 3/8 inch diameter, insulated and heated to 50 °C, was running from the analyser to a backward facing inlet located slightly behind the right cockpit door. A rear-facing inlet was selected to ensure that only vapour (and not particles or droplets) would be collected. A flush pump was used to draw the vapour from outside the aircraft into the cabin through the inlet at a flow rate of about 5 slpm, from which the HIDS2254 was taking a sub-sample in low flow mode. The selected vapour measurements from the aircraft were taken in the lower troposphere above the Iceland sea during a Cold Air Outbreak (CAO) on March 4, 2018. The vapour measurement lasts 9 min and was taken during descent period of the aircraft. Due to a situation of Greenland blocking associated to northerlies in the Greenland-Iceland Seas, the temperature during the flight was low, with an average temperature of -12 °C at altitudes lower than 200 m. Coherent with the low temperatures encountered, the humidity at low levels was ranging from 2'000 to 2'700 ppmv. Even lower humidity (down to about 900 ppmv) was observed at higher levels. Concurrent radiosonde ascent indicated a relative humidity at surface of around 80 % and saturated conditions from 800 to 2'000 m.

For the vapour measurements onboard the research vessel, the analyser HKDS2038 was employed. The analyser was installed inside a heated measurement container which was placed on the boat deck. The ambient air was drawn into the container with a flow rate around 5 slpm by a flush pump through a 5 m long tube. The tube inlet was mounted 4 m above the boat deck, protected from precipitation with a downward facing tin can. The entire tube was maintained at about 50 °C by a heating tape. The selected period from the research vessel was measured during a CAO event between March 14 and 16, 2018. At the beginning of the event, the humidity dropped from 6'000 to below 3'000 ppmv within 2 hours. Then the humidity stayed around 3'000 ppmv for about 24 hours before it increased again to 8'000 ppmv.

3 Isotope composition–humidity dependency

In this section we present the isotope composition–humidity dependence from the characterisation result for instrument HIDS2254. The characterisation is carried out using the method of discrete liquid injections (Sect. 2.2.1). The injections are done by an autosampler, using synthetic air as carrier gas in the vaporizer (experiment 1). During the experiment, in total five standard waters are measured at humidity levels from ∼500 to ∼23'000 ppmv. At each humidity level, totally four injections in high precision mode are applied, where the last three injections are averaged for further analysis. The characterisation result is shown in Fig. 1, with the humidity on the horizontal axis and the isotope composition bias ($\Delta\delta$) on the vertical axis. Note again that all the presented isotope composition biases and humidities are raw measurements.

For the bias on δ^{18}O (i.e. $\Delta\delta^{18}$O), the humidity dependency depicts a tilted and inversed "U" shape (Fig. 1a, symbol). As an example, standard GSM1 (dark blue symbol) starts with a bias of -0.1 ‰ for humidities at 23'000 ppmv, which becomes

https://doi.org/10.5194/amt-2019-316
Preprint. Discussion started: 23 October 2019

Atmospheric Measurement Techniques Discussions

positive after passing 20'000 ppmv until reaching a positive maximum around 3'000 ppmv. Then the bias quickly drops with lower humidity, and becomes negative again around 500 ppmv. As the humidity further decreases, the magnitude of the bias increases substantially. Notably, the humidity dependencies of the other four standard waters (light blue, green, orange, and red symbols for MIX, VATS, DI and EVAP, respectively) also depict a similar tilted and inversed "U" shape. However, the bias maximum becomes smaller and shifts towards the direction of higher humidity (bottom right in Fig. 1a) with more heavy-enriched isotope compositions. This isotope-composition-related shift leads to a substantial increase of the bias difference among the standard waters at the same humidity level. For example, the bias for GSM1 (dark blue symbol) and EVAP (red symbol) differs by ∼0.9 ‰ at 2'000 ppmv, and by ∼2 ‰ at 1'000 ppmv.

The isotope-composition-related shift is even clearer for $\Delta\delta$D (Fig. 1b, symbol). For the standard waters with relatively heavy-depleted isotope compositions (GSM1 (dark blue symbol) and MIX (light blue symbol)), the bias is positive and becomes larger as the humidity decreases. For the standard waters with relatively heavy-enriched isotope compositions (VATS (green symbol), DI (orange symbol) and EVAP (dark red symbol)), the bias goes to more negative values as the humidity decreases. This leads to a divergence of the humidity dependency starting from ∼15'000 ppmv and spreading as the humidity decreases. The bias for GSM1 (dark blue symbol) and EVAP (red symbol) differ by ∼11 ‰ at 2'000 ppmv, and by ∼21 ‰ at 1'000 ppmv.

The isotope-composition-related shift in $\Delta\delta^{18}$O and $\Delta\delta$D results in a substantial shift for the humidity dependency of Δd-excess. The humidity dependency of Δd-excess below ∼15'000 ppmv also depicts an "U" shape. The minimum bias is located at between 4'000 (DI, orange) and 7'000 ppmv (GSM1, dark blue symbol). The bias for GSM1 (dark blue symbol) and EVAP (red symbol) differs by ∼3.8 ‰ at 2'000 ppmv, and by ∼5.3 ‰ at 1'000 ppmv.

In summary, this characterisation shows that the humidity dependence varies systematically according to the isotope composition of the measured standard water. It is most pronounced at low humidity levels (below 10'000 ppmv) and quickly becomes substantial as the humidity further decreases. For example, at a humidity of 1'000 ppmv, failing to account for the dependence on the isotope composition can cause a bias as large as ∼2‰, ∼21 ‰ and ∼5.3 ‰ for δ^{18}O, δD and d-excess, respectively. This is of importance for in situ water vapour measurement in dry environments, in particular where water vapour has largely varying isotope compositions. As is demonstrated in Sect. 6, we find that this isotope composition–humidity dependence persists irrespective of characterizing methods or dry gas supplies, and exists in all three spectrometers investigated here.

This measurement characteristic will not be sufficiently removed by a simple uniform correction of the humidity dependency only. However, the bias can be corrected for if we can establish a correct function of both the humidity and the isotope composition based on the characterisation result. A correction framework dedicated to this purpose is developed in the following section.

https://doi.org/10.5194/amt-2019-316
Preprint. Discussion started: 23 October 2019

Atmospheric Measurement Techniques Discussions

4 Correction framework

In this section, we use the characterisation result from instrument HIDS2254 obtained above as an example on how to derive a correction procedure for the isotope composition–humidity dependence. For the sake of simplicity, we have removed the isotope indicator in the following equations. In other words, the equations in the following are equivalent for δ^{18}O and δD.

1. Measurements: We obtained raw measurements of five standard waters with a range of isotope compositions from -33.07 to 5.03 ‰ and from -262.95 to 4.75 ‰ for δ^{18}O and δD, respectively. The measurements are carried out with discrete liquid injections via an autosampler; the mixing dry gas is synthetic air from a gas cylinder (experiment 1 in Table 2).

2. Data processing: We calculated the deviations of the raw measurements to a reference value at 20'000 ppmv (raw humidity). The reference value is obtained by a linear interpolation between the closest measurements above and below 20'000 ppmv. The deviations are denoted as $\Delta\delta^{18}$O, $\Delta\delta$D and Δd-excess as described in Sect. 2.1 and are used to determine humidity dependency functions.

3. Fitting procedure: (1) Firstly, the characterisation result for each standard water is fitted with a function of the form:

$$f_i(x) = \frac{a_i}{x} + b_i x + c_i, \tag{4}$$

where x is humidity, i indicates one of the standard waters, and a_i, b_i and c_i are fitting coefficients for each standard water.

(2) Then, we plot the obtained coefficients a, b and c for all the standard waters as a function of the isotope composition of the standard waters (Fig. 2, symbols). This reveals a dependence of each fitting coefficient on the isotope composition of the measured water. We approximate this dependence with a quadratic polynomial regression:

$$f_j(y) = m_j(y - n_j)^2 + k_j, \tag{5}$$

where y is isotope composition, j indicates coefficients a, b and c, and m_j, n_j and k_j are fitting coefficients of the quadratic polynomial function.

The obtained coefficients a, b and c in Eq. (4) for the five standard waters measured on instrument HIDS2254 are given in Table 4. Despite the magnitude differs between a, b and c, scaling analysis shows that each of the terms ($\frac{a}{x}$, bx and c) on the right hand side of Eq. (4) contributes similarly to the isotope composition–humidity dependency. The fitting results are shown in Fig. 1 (solid color line). It can be seen that with the choice of this type of function, the behaviour of humidity dependency for both $\Delta\delta^{18}$O and $\Delta\delta$D of each standard water are faithfully captured. Note that the fit for Δd-excess is obtained by calculation. Using the fit of δ^{18}O and δD for each standard water by $\delta_{\text{fit}} = \delta_{\text{ref}} + \Delta\delta_{\text{fit}}$, we first calculate the fit of d-excess for each standard water by the definition $d\text{-excess} = \delta\text{D} - 8 \cdot \delta^{18}\text{O}$. Then, we obtain the fit of Δd-excess by calculating the deviations to the d-excess at the reference humidity level.

The obtained coefficients m, n and k in Eq. (5) are given in Table 5. The fitting results (solid line) with the fitting uncertainty (95 % confidence interval; black dotted line) are shown in Fig. 2. Since we only fit five data points, the fitting

https://doi.org/10.5194/amt-2019-316
Preprint. Discussion started: 23 October 2019

Atmospheric Measurement Techniques Discussions

uncertainty is relatively large, resulting in a relatively large standard deviation for the isotope composition bias ($\Delta\delta$). This large standard deviation for $\Delta\delta$ can be reduced by using a bootstrap approach (Efron, 1979) to estimate the fitting uncertainty in Eq. (5). More details on the bootstrap approach is found in Appendix A.

4. Correction function: The final correction function is obtained as a surface function of both the humidity, x, and the isotope composition of the measured water, y:

$$g(x,y) = \frac{a(y)}{x} + b(y)x + c(y), \tag{6}$$

where $a(y)$, $b(y)$ and $c(y)$ are coefficients determined by the isotope composition of measured water, y.

This results in a two-dimensional correction surface for each isotopologue as shown in Fig. 3 (black contours). Note the denser contour and the increased contour intervals below 4'000 ppmv for both δ^{18}O and δD. For the humidity dependency on both δ^{18}O and δD, the magnitude of the bias increases substantially at low humidities. For δ^{18}O, the bias changes from positive to negative as humidity decreases below ∼4'000 ppmv. For δD, the bias starts to grow below 10'000 ppmv and splits into both positive and negative directions.

The surface function also reflects a clear isotope composition dependence. For example, at the humidity of 2'000 ppmv, the isotope composition bias for a measured water with δ^{18}O of 5 ‰ is about -0.5 ‰, while for a measured water with δ^{18}O of -35 ‰, the bias is about 0.4 ‰. This isotope composition dependence is even more substantial for δD where the humidity dependencies at low humidities diverge with respect to the isotope compositions of the measured waters. The isotope composition bias is negative for a measured water with $\delta\mathrm{D} > -140$ ‰ and positive for a measured water with $\delta\mathrm{D} < -140$ ‰. In addition, the magnitude of the bias increases as δD of the measured water deviates from -140 ‰. At the humidity of 2'000 ppmv, the isotope composition bias spans from ~ -8 ‰ for a measured water with δD of 50 ‰ to ∼8 ‰ for a measured water with δD of -350 ‰. At the same humidity level, the isotope composition bias for δD is about 10 times larger than that for δ^{18}O.

5. Bias correction:

Using the correction function above, given any measured raw humidity and isotope composition within the range investigated here, we can determine the bias and bring the measured isotope compositions to their values at 20'000 ppmv. Thereby, the isotope composition at 20'000 ppmv (δ_{ref}) is the unknown; its analytical solution is found from solving the equation:

$$\delta_{\mathrm{meas}} - \delta_{\mathrm{ref}} = \frac{a(\delta_{\mathrm{ref}})}{h} + b(\delta_{\mathrm{ref}}) \cdot h + c(\delta_{\mathrm{ref}}), \tag{7}$$

where h is the measured raw humidity and δ_{meas} is the measured isotope composition at that humidity level. The right hand side of the equation is the bias determined from Eq. (6). The coefficients $a(\delta_{\mathrm{ref}})$, $b(\delta_{\mathrm{ref}})$ and $c(\delta_{\mathrm{ref}})$ are determined from Eq. (5). Eq. (7) is a quadratic function; the procedure to obtain its analytical solution is given in Appendix B.

https://doi.org/10.5194/amt-2019-316
Preprint. Discussion started: 23 October 2019

Atmospheric Measurement Techniques Discussions

Note that the bias at 20'000 ppmv is not exactly zero because the fit which is based on all the measurements is not constrained to the point [20'000, 0]. Also note that below 500 ppmv the bias has larger uncertainties due to the lack of measurements at this humidity range.

5 Impact of the humidity dependence correction

We now investigate the impact of the humidity dependence correction on datasets from in situ measurements onboard an aircraft and a research vessel presented in Sect. 2.6.

5.1 Correction impact on the aircraft measurements

The low humidities and a relatively wide range of (heavy-depleted) isotope compositions make this profile measurement from aircraft particularly suitable for demonstrating the impact of humidity dependence correction (Fig. 3). During the descent of the aircraft from 2'900 m a.s.l to minimum safe altitude, the measured humidity gradually increases from about 800 ppmv at the top to 2'300 ppmv near the surface (Fig. 4d). The isotope composition profile shows three main characteristics (Fig. 4a, b, c). Above about 1'800 m, δ^{18}O and δD are quite heavy-depleted (around -42 ‰ and -320 ‰ respectively), with *d*-excess being around 10 ‰. Between 1'800 and 1'500 m there is a transition stage where δ^{18}O and δD increase to around -30 ‰ and -270 ‰ respectively, and *d*-excess quickly drops to around -40 ‰. Below 1'500 m, δ^{18}O, δD and *d*-excess gradually increases until reaching around -22 ‰, -170 ‰ and 12 ‰, respectively near the surface.

5.1.1 Comparison of correction schemes

We have created four versions of corrected datasets by applying different humidity dependence correction schemes. The first and second version are corrected for only humidity dependence using the humidity dependency function of standard DI (Fig. 1, orange curve) and standard GSM1 (Fig. 1, dark blue curve), respectively (hereafter referred as *hum-corr-cal-DI* (Fig. 4, orange curve) and *hum-corr-cal-GSM1* (Fig. 4, blue curve). The third version is corrected for both the isotope composition and the humidity dependency using the correction surface in Sect. 4 (hereafter referred as *iso-hum-corr-cal*, black curve with asterisk symbols in Fig. 4). All these three versions are calibrated to VSMOW2-SLAP2 scale after applying the respective humidity dependence correction scheme. The calibration using the VSMOW2-SLAP2 scale for the aircraft dataset is computed using long term SDM measurements of standards GSM1 and DI before and after the flight survey (details described in a forthcoming publication).

The fourth version of the dataset is corrected using an alternative approach that has been applied by Bonne et al. (2014) for their in situ vapour measurements on Greenland. Instead of correcting the humidity dependence for the vapour measurements, their approach corrects the humidity dependence for the measured standards. Thus, assuming the humidity dependencies of the two employed standards remain stable during the measurement period, the measured isotope ratios of these two standards are corrected using humidity dependency function to the ambient air humidity level of each single vapour measurement. Then, the

https://doi.org/10.5194/amt-2019-316
Preprint. Discussion started: 23 October 2019

Atmospheric Measurement Techniques Discussions

linear regression computed from these two corrected standard measurements against their certified values is applied to calibrate the vapour measurement to VSMOW2-SLAP2 scale (hereafter referred as *2-std-hum-corr-cal*, green curve in Fig. 4).

The different correction schemes modify the raw dataset differently. For the δ^{18}O profile, it does not make substantial difference for the measurements below 1'500 m (Fig. 4a). For the measurements above 1'500 m, the version *hum-corr-cal-DI* stands out from the rest by exhibiting a consistent positive offset of about 0.8 ‰. The rest three versions depict similar negative offsets between -0.3 and -0.7 ‰. For the δD profile, a very similar pattern exhibits but with more visible offsets between the correction schemes (Fig. 4b). The disagreement patterns in the corrected δ^{18}O and δD profiles lead to an even stronger offset in the *d*-excess profile (Fig. 4c). We can demonstrate the impacts of the different correction schemes by comparing the four versions of the corrected datasets at the same altitude. Since the impact is most substantial on the measurements above 1'500 m, we choose to use the measurements around 2'600 m as an example in the following.

First, we investigate the impact from applying the correction scheme introduced in this study, i.e., the version *iso-hum-corr-cal*. This version modifies the raw dataset by about -0.4 ‰ and -13.7 ‰ for δ^{18}O and δD, respectively, resulting in a change of about -10.6 ‰ for *d*-excess. Since this version accounts for both the isotope composition dependence and the humidity dependence, hereafter we regard this version as the reference. The impact of applying the reference correction schemes on the aircraft measurements can be understood by examining where the data points align in the correction surface function (Fig. 3, blue crosses). For both δ^{18}O and δD, the data points with low humidity and heavy-depleted isotope compositions cluster in the left bottom corner of the surface function. This is the most sensitive area of the correction, causing thus the largest biases in the surface function.

By comparing the other versions to the reference, we show the different impacts from other correction schemes. The impact of applying the correction scheme accounting for only humidity dependence relies on the choice of the used standard water. In the case of the aircraft dataset here, using the humidity dependency function of standard DI (version *hum-corr-cal-DI*) introduces the largest bias (1.1 ‰, 18.8 ‰ and 9.5 ‰, for δ^{18}O, δD and *d*-excess, respectively). On the contrary, using the humidity dependency function of standard GSM1 (version *hum-corr-cal-GSM1*) produces results that are much closer to the version *iso-hum-corr-cal* (with an offset of 0.1 ‰ and 4.3 ‰ for δ^{18}O and δD, respectively and 3.3 ‰ for *d*-excess). This is due to the fact that the isotope composition of standard GSM1 closely resembles the average isotope composition of the aircraft dataset.

Finally, applying the alternative calibration approach used in Bonne et al. (2014) (*2-std-hum-corr-cal*) results in quite similar profiles to that from the reference version. The version *2-std-hum-corr-cal* is slightly more heavy-depleted, with an offset of about -0.3 ‰ and -0.6 ‰ for δ^{18}O and δD, respectively, resulting in a change of 1.8 ‰ for *d*-excess. The small discrepancy between these two versions are due to the following three factors. Firstly, depending on the number of used standard waters, the interpolation scheme for the bias in between those of the used standard waters can be different. The version *2-std-hum-corr-cal* makes use of the humidity dependency functions of only two standard waters. Therefore the bias can only be linearly interpolated between both standards. In contrast, by measuring five standard waters, the reference version is able to reveal and account for the non-linearity during interpolation. Secondly, the version *2-std-hum-corr-cal* corrects the two standards to the humidity level of the measurement while the reference version corrects the measurement to the humidity level of the

https://doi.org/10.5194/amt-2019-316
Preprint. Discussion started: 23 October 2019

Atmospheric Measurement Techniques Discussions

two standards (i.e. the reference humidity). Based on the humidity dependency feature of the two standards, the choice of correcting the two standards will result in a bigger slope for VSMOW2-SLAP2 calibration line. Consequently, the measurements after calibration is stretched to two ends, i.e., the measurements with isotope composition close to that of standard DI become more heavy-enriched and those close to that of standard GSM1 become more heavy-depleted. Finally, the humidity dependency functions for GSM1 and DI used in the version *2-std-hum-corr-cal* (using the fit of the measurements for GSM1 or DI respectively) are not exactly identical to those used in version *iso-hum-corr-cal* (from the surface function determined by the measurements of five standard waters). Despite the small discrepancy, the consistent results of version *2-std-hum-corr-cal* with the reference version indicate that a correction scheme using humidity dependency functions of only two standard waters covering the measured isotope composition range could be sufficient.

5.2 Correction impact on the ship-based measurements

The same four versions of corrected dataset have been created for the ship measurement. That dataset was calibrated to the VSMOW2-SLAP2 scale using the quasi-daily manual injection measurements of NEEM and GV standards onboard the research vessel.

Applying different correction schemes has a much weaker impact on the vapour measurement onboard the research vessel (not shown). The modification on the raw dataset after applying our isotope composition–humidity dependence correction scheme is on the order of 0.06 and 0.15 ‰ for δ^{18}O and δD, respectively, yielding to a change on the order of -0.5 ‰ for *d*-excess. As can be identified from the location of the red dots in Fig. 3, these data points are located in an area with low sensitivity in the correction surface. This is mainly because these measurements were carried out at the ocean surface with relatively higher humidities (from 2'500 to 8'000 ppmv), but also less heavy-depleted isotope compositions, compared to the aircraft observations. The ocean surface evaporation dominates the isotope compositions which span between -23 to -12 ‰ for δ^{18}O and -160 to -100 ‰ for δD. Essentially, the measurements happen to cluster in a saddle region of the surface function, where the correction function is uniform and small. This indicates that measurements are not under all conditions sensitive to the correction of the isotope composition–humidity dependence. Under conditions where the isotope compositions of vapour vary within a small range or the ambient humidity is relatively high (as shown for aircraft dataset in Sect. 5.1), the bias caused by humidity dependence becomes smaller and a good choice of one or two standard waters representing or covering the measured isotope composition range could be sufficient to correct for the humidity dependence.

6 Stability and robustness

In this section we present the results of stability and robustness tests of the isotope composition–humidity dependence. We address here the possible influence from the choice of the characterisation method, the variation among instruments, the potential instrument drift over time, the type of dry gas supply and the measuring sequence.

https://doi.org/10.5194/amt-2019-316
Preprint. Discussion started: 23 October 2019

Atmospheric Measurement Techniques Discussions

6.1 Vapour generation method

To investigate whether the isotope composition–humidity dependence is influenced by the choice of calibration method, we compare the characterisation result for instrument HIDS2254 using discrete liquid injections and the characterisation result using the SDM (experiment 2, 6). The same standard waters (GSM1 and DI) and dry gas supply (synthetic air) are used in the two experiments. The measurement using the SDM usually has a higher uncertainty since the continuous vapour streaming does not provide entirely constant mixing conditions, and the vapour stream can become unstable due to clogging and bubbles in the capillary. The comparison is shown in Fig. 5. For $\Delta\delta^{18}$O, the humidity dependency determined by discrete liquid injections corresponds well with those determined by the SDM within one standard deviation of the latter, despite a small offset of 0.2–0.5 ‰ for DI between 2'000 and 6'000 ppmv(Fig. 5a). For $\Delta\delta$D, the humidity dependencies for both GSM1 and DI determined by discrete liquid injections are located well within one standard deviation of those determined by the SDM (Fig. 5b). The agreement between the two experiments for $\Delta\delta^{18}$O and $\Delta\delta$D leads to an overall agreement in the calculated Δd-excess (Fig. 5c). A 1–3 ‰ offset between 2'000 to 6'000 ppmv results from the offset in $\Delta\delta^{18}$O in the same humidity range.

Comparison of the two vapour generation methods using N_2 as dry gas supply (experiment 3 and 8) also gives a similar isotope composition–humidity dependence for both methods (not shown), confirming that the isotope composition–humidity dependence does not depend substantially on either of the two tested methods to generate standard water vapour.

6.2 Variations among CRDS analysers

To investigate the variations of the humidity dependency between the individual instruments, we have repeated the same characterisation on three analysers (experiment 3, 9 and 13). The characterisation is carried out with four standard waters (GSM1, VATS, DI and EVAP), using liquid injections via an autosampler with N_2 as the mixing dry gas. The characterisation results for the three analysers are shown in Fig. 6.

For $\Delta\delta^{18}$O, the positive bias for GSM1 below 4'000 ppmv on instrument HKDS2038 is about 0.2–1.8 ‰ stronger than those on the other two analysers (Fig. 6a, d, g, blue). The humidity dependency of VATS below 4'000 ppmv is nearly flat on instrument HKDS2038 while exhibiting a substantially negative bias on the other two analysers. The humidity dependencies for the other two standard waters (DI and EVAP) are in good agreement among the three analysers. For $\Delta\delta$D, the humidity dependency of VATS below 2'000 ppmv is slightly positive on instrument HKDS2038 while being nearly flat on the other two analysers (Fig. 6b, e, h, green). The humidity dependency for the other three standard waters (GSM1, DI and EVAP) agree well among the three analysers. The calculated d-excess (Fig. 6c, f, i) shows an increasing positive bias towards the low end of humidity for almost all standard waters measured on the three analysers, except for DI and GSM1 measured on instrument HKDS2038, whose humidity dependencies appear to be rather flat or even slightly negative.

Despite of the minor differences of the bias, it is clear that the isotope composition–humidity dependency exists in all three analysers investigated here. The behaviour of dependency is to the first order in good agreement across the analysers. For the standard waters with relatively heavy-depleted isotope compositions, the measurements on all the three analysers exhibit

https://doi.org/10.5194/amt-2019-316
Preprint. Discussion started: 23 October 2019


Atmospheric Measurement Techniques Discussions

a humidity dependency where the measured isotope composition becomes more heavy-enriched as the humidity decreases. For the standard waters with relatively heavy-enriched isotope compositions, the measurements exhibit a reversed humidity dependency.

6.3 Long term stability

To quantify the long term stability of the isotope composition–humidity dependency, we examine the temporal change of the fitting coefficients (a_i, b_i and c_i) in Eq. (4). The change over time is considered insignificant if it is within the 95 % confidence bounds for the fitted curve. Figure 7 shows the fitting coefficients for the humidity dependency characterised by liquid injections on instrument HIDS2254 in February 2017 (black line, experiment 1) and in May 2018 (red line, experiment 2). For the characterisation in May 2018, only four standard waters are measured. This results in a fit with a relatively large 95 % confidence interval. In this context, the change over time is considered insignificant if the coefficients (and their fitted curve) from the characterisation in May 2018 is within the 95 % confidence bounds for the fitted curve from the characterisation in February 2017.

For the humidity dependency on δ^{18}O, the change of coefficient a is insignificant. However, it is worth to note that the fitting coefficient a with respect to standard GSM1 (Fig. 7a, the first data point) changes slightly from negative to positive. This small change results in an opposite humidity dependency shape at low humidity level. The change of the humidity dependency for GSM1 reflects partly on the sensitivity of the instrument on a certain range of isotope composition and partly on the uncertainty arising from both low instrument precision and lack of measurements at low humidities. The change of coefficients b and c are substantial for waters of relatively heavy-enriched δ^{18}O (Fig. 7b, c). A less negative b and a less positive c reflects a weaker humidity dependency in May 2018. The humidity dependency on δD shows reasonable agreement for all three fitting coefficients (Fig. 7d, e, f), and points to the same basic shape of the humidity dependency on δD after a 15 month period.

A repeated characterisation with standard water DI via SDM in July 2016 (experiment 4), February 2018 (experiment 5) and June 2018 (experiment 6) indicates that the humidity dependency for standard water DI is still consistent after nearly two years (not shown). The humidity dependencies of the three standard waters (GSM1, VATS and DI) determined by liquid injections via an autosampler (experiment 9 and 10) and the three standard waters (NEEM, GV and BERM) via manual injections on instrument HKDS2038 indicates a consistent isotope composition–humidity dependency after a running of one year and one month, respectively (not shown). Overall, the stability tests indicate that the isotope composition–humidity dependency of each analyser is to first order stable on a long term basis (1–2 years).

6.4 Influence of dry gas supply

Next, we investigate whether the type of the dry gas supply has an influence on the characterisation results. To this end, we test the characterisation method via SDM on instrument HIDS2254 with a supply of synthetic air, a supply of N_2 and a supply of dried ambient air through Drierite (experiment 6–8). The synthetic air and N_2 are tested with two standard waters (GSM1 and DI), and the Drierite is tested with one standard water (GSM1).

https://doi.org/10.5194/amt-2019-316
Preprint. Discussion started: 23 October 2019

Atmospheric Measurement Techniques Discussions

For humidity dependency on $\delta^{18}O$, the measurement with Drierite disagrees strongly from those with synthetic air and N_2 (Fig. 8a). As humidity decreases below about 7'000 ppmv, the measured GSM1 with Drierite exhibits a fast increasing positive bias while those with synthetic air and N_2 exhibit a rather flat dependency. The measurements with synthetic air and with N_2 show a largely similar shape. A small discrepancy exists below 15'000 ppmv, where both standard waters measured with N_2 exhibit a small negative offset ($\sim$0.5‰). The humidity dependencies on δD from all three types of the dry gas supply are in good agreement, despite a small ($<$1.5‰) offset between the measurement with synthetic air and that with N_2 (Fig. 8b). The calculated *d*-excess follows the shape of $\delta^{18}O$, with a different behaviour between the measurement with Drierite and those with synthetic air and N_2 below about 7'000 ppmv (Fig. 8c). The *d*-excess of the experiment with N_2 exhibits a small positive offset ($\sim$0.5‰) compared to that of measurement with synthetic air. Overall, characterisation results with synthetic air and N_2 exhibit a humidity dependency in a good agreement for both standard waters (GSM1 and DI). However, the characterisation result (for GSM1) with the Drierite differ significantly in $\delta^{18}O$ and thus also *d*-excess.

The characterisation method of liquid injections via an autosampler is also tested with synthetic air and N_2. Again, the results exhibit a similar isotope composition–humidity dependency from the two types of dry gas supply, despite a discrepancy for $\delta^{18}O$ measured with N_2 in the dependency for GSM1 below 2'000 ppmv and a larger negative offset (0.5–1.3‰) for DI below 10'000 ppmv (not shown). A test of synthetic air from a gas cylinder and dried ambient air from Drierite in the study of Aemisegger et al. (2012) also shows that the humidity dependency for $\delta^{18}O$ is different while being more similar for δD. The observed discrepancy in the $\delta^{18}O$ bias is possibly due to changes in the baseline of the spectrum around the $\delta^{18}O$ (i.e., $^1H_2^{18}O$ and $^1H_2^{16}O$) absorption peak, caused by slight differences in trace gas composition (Aemisegger et al., 2012; Rella et al., 2015).

6.5 Influence from the measuring sequence

Finally, we investigate whether a measuring sequence with ascending or descending humidity sequence influences humidity dependency characterisation. The humidity dependencies of GSM1, MIX and DI tap water characterised with ascending and descending humidity sequences are shown in Fig. 9. For $\Delta\delta^{18}O$ (Fig. 9a), the humidity dependency from the two humidity sequences overall agree well for DI tap water (orange symbol and curve). The measurements for GSM1 with the descending humidity sequence (dark blue symbol and curve) exhibit a weaker humidity dependency below about 5'000 ppmv. However, the measurements for MIX below 2'000 ppmv (light blue symbol and curve) exhibit an interesting contrast. The measurement at the lowest humidity level (around 500 ppmv) has constrained the humidity dependency into opposite directions. The case for $\Delta\delta$D (Fig. 9b) is more uniform among the three tested waters. The results from the two measuring sequences are in good agreement, with a slightly but systematically weaker humidity dependency by the descending humidity sequence. The combination of the disagreement in $\Delta\delta^{18}O$ and the weaker dependency in $\Delta\delta$D results in various humidity dependencies for Δd-excess (Fig. 9c). For example, the results for DI tap water overall agree between the two sequences. However, the results for GSM1 exhibit contrary humidity dependencies.

In general, the measurements from descending humidity sequence exhibit slightly weaker humidity dependencies. One possible, but unlikely, explanation is the memory effect from moisture remaining from previous injections (even after flushing the system with 12 injections at 20'000 ppmv), which would still play a role during the characterisation measurements. If this

https://doi.org/10.5194/amt-2019-316
Preprint. Discussion started: 23 October 2019

Atmospheric Measurement Techniques Discussions

is the case, starting the measurements with injections of higher humidity levels at the beginning (i.e., descending humidity sequence) would help to overwrite the memory from the previous samples.

The contrast $\Delta\delta^{18}O$ measurement at about 500 ppm for MIX is not well understood, since it cannot be explained by a memory effect[1], and errors in data handling and processing have been ruled out. The uncertainty in the dependency shape of MIX is likely due to the uncertain dependency at this range of isotope compositions, where the dependency is between strongly heavy-depleted water (GSM1) and other relatively heavy-enriched waters. This can be also found, for example, in the small shift of dependency shape in δD for VATS among the three analysers (Fig. 6b, e, h, green curve). Further tests with more standards or a vapour generation approach that do not suffer from memory is needed to address this uncertainty in the dependency shape.

7 Discussion

The isotope composition–humidity dependency appears as a robust feature of current-generation stable water isotope analysers of the Picarro brand. In a careful characterisation for low humidities, it is apparently independent of vapour generation method, instrument type and dry gas supply, to first order constant over several years, and independent of measuring sequence. Here we further discuss the possible causes of the isotope composition–humidity dependency. In particular, we explore whether the isotope composition–humidity dependency is an artefact from mixing with water remaining within the analyser, or an instrument behaviour resulting from spectroscopic or other design characteristics.

If we assume the dependency is a result from mixing with remnant water, there would be mainly two candidates of the background moisture source: (1) the remaining water vapour in the dry gas supply; (2) the remaining water vapour from previous measurement. By changing the dry gas supply from the ambient air dried through Drierite to synthetic air or N_2 from cylinder which typically provides a dry gas with a humidity below 10 ppmv, we can exclude the possible influence from the background moisture in the dry gas supply. In order to quantify the amount and the isotope compositions of the remaining water vapour from previous measurement, we have applied several successive *empty injections* via the autosampler. Thereby, no liquid is injected, and only dry gas is flushed into the vaporizer, and mixed with any remnant moisture in the analyser system. Results from these empty injections show that the remaining water vapour in the system typically has a humidity of about 60–80 ppmv, with its isotope composition closely following those of the previous injections. If the humidity dependency were a result of the mixing between the injected water and the remaining water vapour from previous measurement, by injecting the same standard water during a characterisation run, we would expect a mixing of two water vapour masses of same isotope compositions at different humidities. As a consequence, we would expect the mixed vapour to have the same isotope compositions, which is not the case. Finally, the shape of the isotope composition–humidity dependency with a maximum between 2'000 and 6'000

[1]This is because the instrument has been shut down for two weeks before running the measurement for MIX. The last measurement from two weeks ago was standard EVAP which is more heavy-enriched than MIX. If the disagreement between the results are caused by the memory from remaining EVAP sample in the system, the measurement should reflect that already in the ascending sequence (leading to positive $\Delta\delta$ values at low humidities) since the ascending sequence is measured before descending sequence. However, the measurements from ascending sequence exhibit a negative bias while those from the descending sequence exhibit a positive bias.

https://doi.org/10.5194/amt-2019-316
Preprint. Discussion started: 23 October 2019


Atmospheric Measurement Techniques Discussions

ppmv (Fig. 1a) is not consistent with the expectation of a memory effect what would monotonously increase with decreasing humidity.

This leaves the second hypothesis to be explored further, namely that the isotope composition–humidity dependency is an instrument behaviour resulting from spectroscopic or other design characteristics. Spectroscopic effects can originate from low absorption at low water molecule concentrations in the cavity. Under such dry conditions, the fitting of absorption peak has a bigger uncertainty (Rella et al., 2015). While a full investigation of the actual physical reasons is beyond the scope of this manuscript, we note that the manufacturer recommends to either measure the standard water and the sample at the same concentrations, or to include at least two concentrations at the same (or similar) isotope composition in the calibration regime so that the non-linear concentration dependency can be quantified over time (Picarro, 2017).

Our study is currently limited by the limited range of the standard waters used here ($-33\sim5$ ‰ and $-263\sim5$ ‰ for δ^{18}O and δD, respectively). Depending on the measurement environment, more heavy-depleted (such as Antarctic inland snow) or heavy-enriched standards would be needed to derive a correction function over the entire measurement range of samples. A clear limitation of the characterisations performed here is the high time demand. The characterisation method with liquid injections provides relatively high precision performance but requires an autosampler and takes about 1–2 weeks for four standard waters. The characterisation method with a SDM can be automated more easily, but requires manual intervention to apply more than two standards. A device that could provide any desired isotope composition and a given humidity level would be needed to fully automate the isotope composition–humidity dependency of the instruments tested here.

8 Final remarks and recommendations

We have systematically investigated the humidity dependency of water vapour isotope measurements for three commercially available infra-red cavity ring-down spectrometers. We found that the humidity dependency varies with the isotope composition of the measured vapour. We define this behaviour as isotope composition–humidity dependency. Using the characterisation results of five standard waters on a Picarro L2130-i as an example, we show how a bias correction scheme for this isotope composition–humidity dependency can be developed. Using the correction scheme, we can determine and correct the isotope composition bias for any measured humidity and isotope composition within the range investigated here and report all the measured isotope compositions at the same humidity level (e.g., 20'000 ppmv in this study).

To demonstrate the impact of the humidity dependency correction, we have compared the developed correction scheme with the correction schemes from the published literature, using in situ measurements from cold and dry environments. The impact is found to be most substantial on the measurements at the lowest humidity levels (below 1'600 ppmv). Applying a correction scheme accounting for only humidity dependency relies on the choice of the used standard water. For an aircraft dataset, using the humidity dependency function based on the standard DI produces a large deviation from the reference profile, while using the humidity dependency based on standard GSM1 produces profiles similar to the reference, since it is closer to the average isotope composition of the aircraft dataset. Finally, we have investigated the impact of applying a correction scheme used by Bonne et al. (2014). This approach produces results in good agreement with that from our approach. The small discrepancy is

https://doi.org/10.5194/amt-2019-316
Preprint. Discussion started: 23 October 2019

Atmospheric Measurement Techniques Discussions

due to the scheme of bias interpolation (linear or non linear), the choice of correcting humidity dependency of the standards or that of the vapour measurement and the small discrepancy in the humidity dependency functions of the two standards. The consistent results indicate that a correction scheme using humidity dependency functions of only two standards covering the isotope composition could be sufficient if the correction surface can be sufficiently approximated by linear interpolation. Using ship measurements made at higher humidity conditions, we find a weaker impact from the different correction schemes.

We have further evaluated the stability and robustness of the isotope composition–humidity dependency regarding the vapour generation methods, the variation among the instruments, the possible long term drift, the type of dry gas supplies and the measuring sequence. The robustness test indicates that the isotope composition–humidity dependency is consistent disregarding the two vapour generation methods, i.e., discrete liquid injections and continuous vapour streaming. It is clear that this isotope composition–humidity dependency exists in a similar fashion in all three investigated analysers. Repeated characterisations during a 1–2 year time period show that the isotope composition–humidity dependency is an instrument characteristic that is to the first order constant. Characterisations with synthetic air and N_2 are similar, while results using Drierite differ substantially in $\delta^{18}O$, likely due to the mixing effect from the remaining moisture after the dry unit. The measuring sequence from high to low or revers shows slightly differing results, pointing to potentially unresolved issues in the vapour generation method. We suspect this is most likely due to the high sensitivity of the humidity dependency at this range of $\delta^{18}O$ values.

In the end, we have discussed the possible origin of the robust isotope composition–humidity dependency. We have excluded the possible mixing effect from the remaining moisture in the dry gas supply and that from previous injections. Even though a full investigation of the physical reason is beyond the scope of this manuscript, we propose that the isotope composition–humidity dependency is to first order a constant instrument characteristic. It probably has a spectroscopic origin, resulting from a larger uncertainty in the fitting of absorption peak at low water molecular concentrations (Rella et al., 2015).

The correction for the isotope composition–humidity dependency is most relevant for in situ vapour isotope measurements where the ambient humidity is low (below 4'000 ppmv) and the isotope composition of measured vapour spans a large range. At higher humidities, Picarro analysers show negligible dependency on either the humidity or the isotope composition. If the isotope composition of ambient vapour varies in a small range during the sampling period, a simpler correction scheme could be employed, using the humidity dependency of two or even one suitable standard water with a similar isotope composition as that of ambient vapour.

Based on our conclusions above, we recommend the following procedures for the correction of the isotope composition–humidity dependency for in situ vapour isotope measurements using Picarro infra-red laser spectrometers. The procedures are particularly relevant for those measurements under cold and dry conditions (with a humidify below 4'000 ppmv) and subject to a relatively large variation in the isotope compositions, such as during aircraft experiments.

(1) A correction scheme with a surface function should be established for each individual instrument according to the characterisation results from the multiple standard waters following the procedures in this paper.

https://doi.org/10.5194/amt-2019-316
Preprint. Discussion started: 23 October 2019


Atmospheric Measurement Techniques Discussions

(2) Even though the isotope composition–humidity dependency appears at first order similar across the three analysers, the detailed shape can vary from instrument to instrument. We recommend to characterise each individual instrument to obtain a specific correction function.

(3) Five or more standard waters that span the full range of ambient vapour isotope compositions should be used to determine the isotope composition–humidity dependency surface.

(4) While the isotope composition–humidity dependency was found to be overall stable within a period of one year for the instruments investigated here, we recommended to repeat the characterisation at least every 6–12 months to capture the possible change in humidity dependency behaviour.

(5) If the measurements of multiple standard waters are not available, the approach used in Bonne et al. (2014) could be applied as an alternative correction approach. Their approach can produce similar results as that from the approach proposed here, but requires the characterisation of the humidity dependency of two carefully selected calibration standards in a linear range of the correction surface. If the isotope composition of ambient vapour varies only within a small range during the sampling period, such as during measurements close to the ocean surface, it may be sufficient to correct for the humidity dependency using one standard water that has a similar isotope composition as that of ambient vapour.

A reproducible and accepted characterisation method is of utmost importance for comparing measurements across disparate locations and in bottom-up networks, in particular in the polar regions, and appears as a prerequisite for detecting representative signals in the stable isotope record on a regional scale. In particular studies employing the d-excess as an indicator of moisture origin or other tracer applications are therefore likely to profit from a detailed characterisation of their analysers according to our characterisation procedure, either before, during or after field deployments.

Code and data availability. Available from the authors on request.

Appendix A: Fitting uncertainty estimated using a bootstrap approach

Since we only have 5 available data points to fit in Eq. (5), the resulted 95 % confidence interval of the fit is relatively broad (black dotted line, Fig. 2). This broad confidence interval results in a relatively large standard deviation for the isotope composition bias ($\Delta\delta$). For example, the resulted standard deviation for $\Delta\delta$ at 2'000 ppmv is about 0.20, 2.69 and 3.13 ‰ for δ^{18}O, δD and d-excess, respectively. To reduce this large standard deviation for $\Delta\delta$, we use a bootstrap approach (Efron, 1979) to estimate the fitting uncertainty in Eq. (5).

The bootstrap approach can be explained by considering for example the coefficient a. Firstly, for each individual observation of a, we generate 1'000 random values under a normal distribution with the mean and standard deviation being those of each available observation. We obtain now five sets of 1'000 random values since we have five a from five standard waters. Then, we sample one value from each set of the 1'000 random values and fit those sampled five values using Eq. (5). Finally, we

https://doi.org/10.5194/amt-2019-316
Preprint. Discussion started: 23 October 2019

Atmospheric Measurement Techniques Discussions

repeat this process 1'000 times, thus obtain 1'000 fits. The standard deviation of the 1'000 fits is the standard deviation that is adopted here (blue dotted line, Fig. 2).

In this way, the standard deviations estimated for the coefficients sa, b and c are lowered to about 15, 0.4×10^{-6} and 8×10^{-3} for δ^{18}O and 100, 3×10^{-6} and 0.1 for δD, respectively. This in turn substantially reduces the resulted standard deviation for $\Delta\delta$. For example, the standard deviation for $\Delta\delta$ at 2'000 ppmv is reduced by a factor of 20, being about 0.01, 0.11 and 0.14 ‰ for δ^{18}O, δD and d-excess, respectively.

Appendix B: Analytical solution for δ_{ref}

In the following we derive the analytical solution for δ_{ref} in Eq. (7) at a reference humidity q_{ref} =20'000 ppmv. The derivation applies for both δ^{18}O and δD.

The coefficients a(δ_{ref}), b(δ_{ref}) and c(δ_{ref}) are given according to Eq. (5):

$$\begin{cases} a(\delta_{\text{ref}}) = m_a(\delta_{\text{ref}} - n_a)^2 + k_a, \\ b(\delta_{\text{ref}}) = m_b(\delta_{\text{ref}} - n_b)^2 + k_b, \\ c(\delta_{\text{ref}}) = m_c(\delta_{\text{ref}} - n_c)^2 + k_c, \end{cases} \tag{B1}$$

Substitute Eq. (B1) into Eq. (7) and rearrange the terms, we get:

$$A\delta_{\text{ref}}^2 + B\delta_{\text{ref}} + C = 0, \qquad \text{where} \begin{cases} A = \dfrac{m_a}{h} + m_b h + m_c, \\ B = 1 - \dfrac{2m_a n_a}{h} - 2m_b n_b h - 2m_c n_c, \\ C = \dfrac{m_a n_a^2}{h} + m_b n_b^2 h + m_c n_c^2 + \dfrac{k_a}{h} + k_b h + k_c - \delta_{\text{meas}}, \end{cases} \tag{B2}$$

Eq. (B2) is a quadratic equation with its only physical solution being:

$$\delta_{\text{ref}} = \frac{-B + \sqrt{B^2 - 4AC}}{2A}. \tag{B3}$$

The coefficients m, n and k are already obtained from the fits in Eq. (5). When given a measured humidity, h, and the corresponding isotope composition, δ_{meas}, we can obtain the isotope composition at q_{ref} =20'000 ppmv, δ_{ref}, according to the solution Eq. (B3).

Competing interests. The authors declare that no competing interests are present in this study.

Acknowledgements. We thank Iris Thurnherr, Franziska Aemisegger and Pascal Graf from the Institute for Atmospheric and Climate Sciences, ETH Zurich, Hans Christian Steen-Larsen and Sonja Wahl from the Geophysical Institute, University of Bergen, Jean-Lionel Lacour and Tomas Foldes, for valuable discussions. Thanks for Árný Erla Sveinbjörnsdóttir from the Isotope Laboratory of University of Iceland

https://doi.org/10.5194/amt-2019-316
Preprint. Discussion started: 23 October 2019

Atmospheric Measurement Techniques Discussions

for providing the UI standard waters. Jarle Berntsen from the Department of Mathematics at University of Bergen is acknowledged for helping to identify a suitable fitting function. We are grateful to the scientists and other personnel who made the measurements during the Iceland-Greenland Seas campaign in 2018 possible. This publication received funding from the Research Council of Norway through Projects SNOWPACE (Contract no. 262710) and FARLAB (Contract no. 245907).

https://doi.org/10.5194/amt-2019-316
Preprint. Discussion started: 23 October 2019

Atmospheric Measurement Techniques Discussions

References

Aemisegger, F., Sturm, P., Graf, P., Sodemann, H., Pfahl, S., Knohl, A., and Wernli, H.: Measuring variations of δ^{18}O and δ^{2}H in atmospheric water vapour using two commercial laser-based spectrometers: an instrument characterisation study, Atmos, Meas. Tech, 5, 1491–1511, 2012.

Bailey, A., Noone, D., Berkelhammer, M., Steen-Larsen, H. C., and Sato, P.: The stability and calibration of water vapor isotope ratio measurements during long-term deployments, Atmospheric Measurement Techniques, 8, 4521–4538, https://doi.org/10.5194/amt-8-4521-2015, 2015.

Bastrikov, V., Steen-Larsen, H. C., Masson-Delmotte, V., Gribanov, K., Cattani, O., Jouzel, J., and Zakharov, V.: Continuous measurements of atmospheric water vapour isotopes in western Siberia (Kourovka), Atmospheric Measurement Techniques, 7, 1763–1776, https://doi.org/10.5194/amt-7-1763-2014, 2014.

Bonne, J.-L., Masson-Delmotte, V., Cattani, O., Delmotte, M., Risi, C., Sodemann, H., and Steen-Larsen, H.: The isotopic composition of water vapour and precipitation in Ivittuut, southern Greenland, Atmospheric Chemistry and Physics, 14, 4419–4439, 2014.

Bonne, J.-L., Behrens, M., Meyer, H., Kipfstuhl, S., Rabe, B., Schönicke, L., Steen-Larsen, H. C., and Werner, M.: Resolving the controls of water vapour isotopes in the Atlantic sector, Nature communications, 10, 1632, 2019.

Crosson, E. R.: A cavity ring-down analyzer for measuring atmospheric levels of methane, carbon dioxide, and water vapor, Applied Physics B-Lasers And Optics, 92, 403–408, 2008.

Dansgaard, W.: The abundance of O18 in atmospheric water and water vapour, Tellus, 5, 461–469, 1953.

Dansgaard, W.: The O18-abundance in fresh water, Geochimica et Cosmochimica Acta, 6, 241–260, http://www.sciencedirect.com/science/article/B6V66-488Y5HP-1V6/2/e7ca8aaef7549373eab07d45b525387c, 1954.

Dansgaard, W.: Stable isotopes in precipitation, Tellus, 16, 436–468, 1964.

Efron, B.: Bootstrap Methods: Another Look at the Jackknife, Annals of Statistics, 7, 1–26, 1979.

Gat, J. R.: Oxygen and hydrogen isotopes in the hydrologic cycle, Annual Review of Earth and Planetary Sciences, 24, 225–262, 1996.

IAEA: Reference Sheet for VSMOW2 and SLAP2 international measurement standards, 2009.

Kerstel, E.: Isotope ratio infrared spectrometry, in: Handbook of stable isotope analytical techniques, pp. 759–787, Elsevier, 2004.

Kerstel, E. and Gianfrani, L.: Advances in laser-based isotope ratio measurements: selected applications, Applied Physics B-Lasers And Optics, 92, 439–449, 2008.

Lis, G., Wassenaar, L., and Hendry, M.: High-precision laser spectroscopy D/H and 18O/16O measurements of microliter natural water samples, Analytical chemistry, 80, 287–293, 2008.

Picarro: Calibration guide for Picarro analyzers, Rev 1., pp. 7–9, 2017.

Rella, C. W., Hoffnagle, J., He, Y., and Tajima, S.: Local- and regional-scale measurements of CH_4, $\delta^{13}CH_4$, and C_2H_6 in the Uintah Basin using a mobile stable isotope analyzer, Atmospheric Measurement Techniques, 8, 4539–4559, https://doi.org/10.5194/amt-8-4539-2015, https://www.atmos-meas-tech.net/8/4539/2015/, 2015.

Renfrew, I., Pickart, R., Våge, K., Moore, G., Bracegirdle, T., Elvidge, A., Jeansson, E., Lachlan-Cope, T., McRaven, L., Papritz, L., et al.: The Iceland Greenland Seas Project, Bulletin of the American Meteorological Society, 2019.

Schmidt, M., Maseyk, K., Lett, C., Biron, P., Richard, P., Bariac, T., and Seibt, U.: Concentration effects on laser-based δ^{18}O and δ^{2}H measurements and implications for the calibration of vapour measurements with liquid standards, Rapid Communications in Mass Spectrometry, 24, 3553–3561, 2010.

https://doi.org/10.5194/amt-2019-316
Preprint. Discussion started: 23 October 2019

Sodemann, H., Aemisegger, F., Pfahl, S., Bitter, M., Corsmeier, U., Feuerle, T., Graf, P., Hankers, R., Hsiao, G., Schulz, H., et al.: The stable isotopic composition of water vapour above Corsica during the HyMeX SOP1 campaign: insight into vertical mixing processes from lower-tropospheric survey flights, Atmospheric Chemistry and Physics, 17, 6125–6151, 2017.

Steen-Larsen, H. C., Johnsen, S. J., Masson-Delmotte, V., Stenni, B., Risi, C., Sodemann, H., Balslev-Clausen, D., Blunier, T., Dahl-Jensen, D., Ellehoj, M. D., Falourd, S., Grindsted, A., Gkinis, V., Jouzel, J., Popp, T., Sheldon, S., Simonsen, S. B., Sjolte, J., Steffensen, J. P., Sperlich, P., Sveinbjornsdottir, A. E., Vinther, B. M., and White, J. W. C.: Continuous monitoring of summer surface water vapor isotopic composition above the Greenland Ice Sheet, Atmospheric Chemistry and Physics, 13, 4815–4828, https://doi.org/10.5194/acp-13-4815-2013, 2013.

Steen-Larsen, H. C., Sveinbjörnsdottir, A. E., Peters, A. J., Masson-Delmotte, V., Guishard, M. P., Hsiao, G., Jouzel, J., Noone, D., Warren, J. K., and White, J. W. C.: Climatic controls on water vapor deuterium excess in the marine boundary layer of the North Atlantic based on 500 days of in situ, continuous measurements, Atmospheric Chemistry and Physics, 14, 7741–7756, https://doi.org/10.5194/acp-14-7741-2014, 2014.

Sturm, P. and Knohl, A.: Water vapor δ^2H and δ^{18}O measurements using off-axis integrated cavity output spectroscopy, Atmospheric Measurement Techniques, 3, 67–77, 2010.

Wen, X. F., Lee, X., Sun, X. M., Wang, J. L., Tang, Y. K., Li, S. G., and Yu, G. R.: Intercomparison of four commercial analyzers for water vapor isotope measurement, Journal of Atmospheric and Oceanic Technology, 29, 235–247, https://doi.org/10.1175/JTECH-D-10-05037.1, 2012.

https://doi.org/10.5194/amt-2019-316
Preprint. Discussion started: 23 October 2019

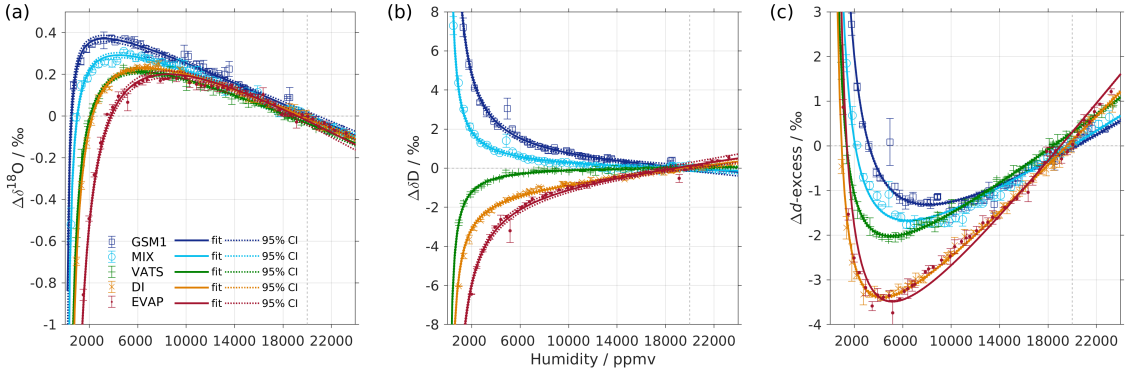

Figure 1. Humidity dependency of uncalibrated measurements for **(a)**: δ^{18}O, **(b)**: δD and **(c)**: d-excess. Humidity dependency is expressed as the deviation Δ of the measured isotope composition at each humidity with respect to the reference humidity of 20'000 ppmv for five standard waters (GSM1, MIX, VATS, DI and EVAP) on instrument HIDS2254 (Picarro L2130-i) with discrete liquid injections via an autosampler (experiment 1). Symbol and error bar represents the mean and the standard deviation of the last three of four injections. Solid lines are fits with the function $f(x) = \frac{a}{x} + bx + c$. Dashed lines are the 95 % confidence interval for the corresponding fit. Measurements and fits for d-excess are calculated from $d\text{-excess} = \delta\text{D} - 8 \cdot \delta^{18}\text{O}$. Two outliers (at about 4'300 and 8'900 ppmv) are removed from GSM1 measurements and one outlier (at about 9'000 ppmv) is removed from VATS measurements.

https://doi.org/10.5194/amt-2019-316
Preprint. Discussion started: 23 October 2019

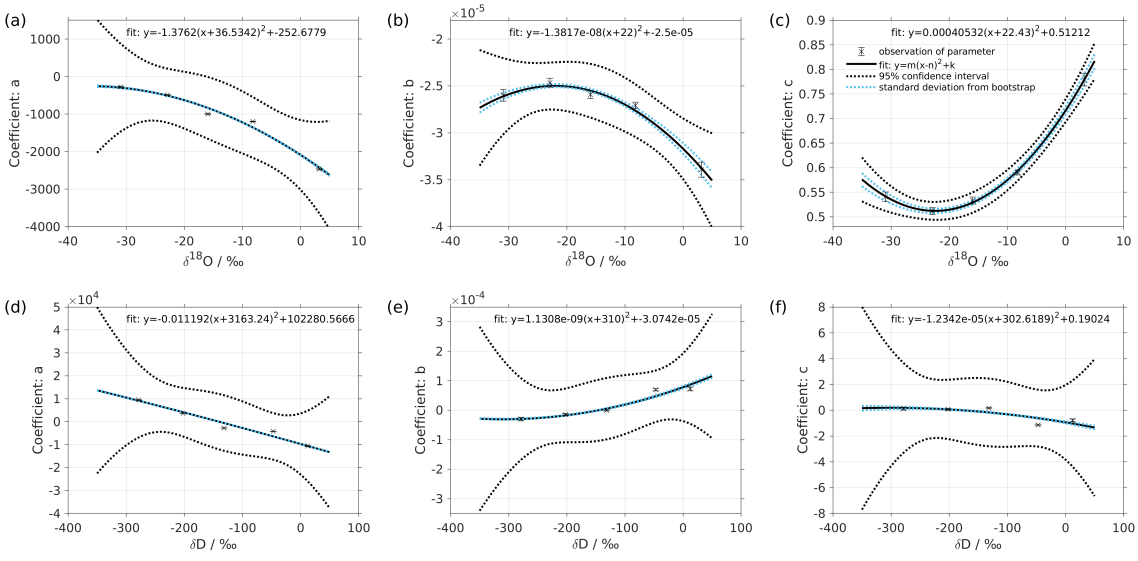

Figure 2. Dependency of fitting coefficients a, b and c on δ^{18}O **(a)–(c)** and on δD **(d)–(f)**. The coefficients a, b and c are from the fits for the five standard waters in Fig. 1. Solid line is the quadratic fit with $f_j(y) = m_j(y - n_j)^2 + k_j$. Black dotted line shows the 95 % confidence interval. Blue dotted line shows the standard deviation estimated from a bootstrap method.

https://doi.org/10.5194/amt-2019-316
Preprint. Discussion started: 23 October 2019

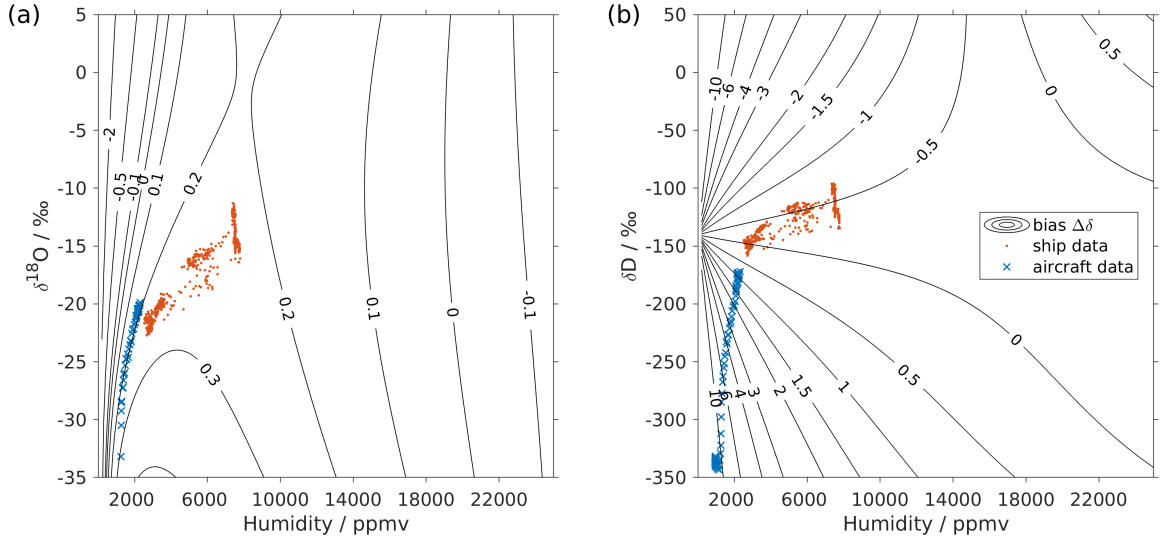

Figure 3. Surface function of the bias for **(a)** δ^{18}O and **(b)** δD, based on the isotope composition–humidity dependency of instrument HIDS2254 (Picarro L2130-i). The x-axis is the raw humidity and y-axis shows the raw isotope composition at 20'000 ppmv. Contours with numbers indicate the isotope composition bias, $\Delta\delta$. Symbols show the isotope measurements during cold and dry conditions over the Iceland Sea: measurements in every 10 seconds from an aircraft in the lower troposphere (blue crosses) and in every 10 minutes from a research vessel on the ocean surface (red dots). The measurements from the aircraft were done with instrument HIDS2254 (Picarro L2130-i) and those on the research vessel were done with instrument HKDS2038 (Picarro L2140-i).

https://doi.org/10.5194/amt-2019-316
Preprint. Discussion started: 23 October 2019

Atmospheric Measurement Techniques Discussions

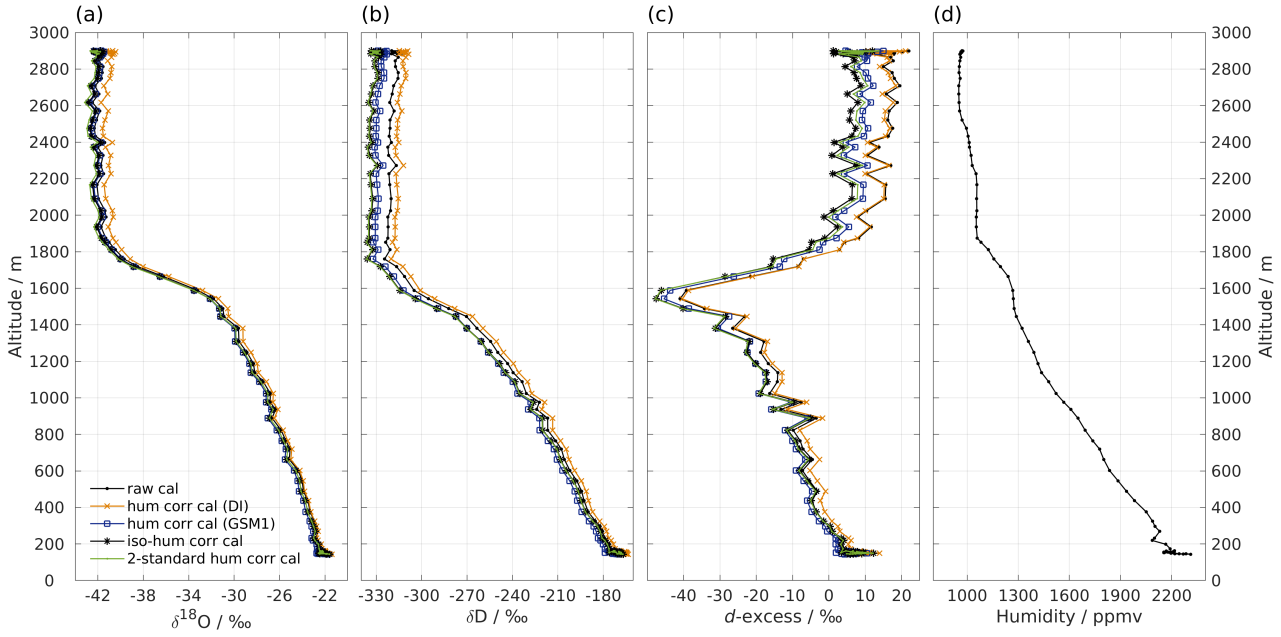

Figure 4. Vertical profiles of **(a)** δ^{18}O, **(b)** δD, **(c)** *d*-excess and **(d)** humidity measured by instrument HIDS2254 on an aircraft above the Iceland Sea on Mar 04, 2018. Shown are profiles of the raw dataset (black curve with dot) and four datasets using different isotope composition–humidity dependency correction schemes: using the humidity dependency of standard DI (orange curve with cross), standard GSM1 (blue curve with square), the isotope composition–humidity dependency surface function (black curve with asterisk), and using two humidity-dependency-corrected standards (green curve with dot). All the shown datasets are calibrated to VSMOW2-SLAP2 scale.

https://doi.org/10.5194/amt-2019-316
Preprint. Discussion started: 23 October 2019

Atmospheric Measurement Techniques Discussions

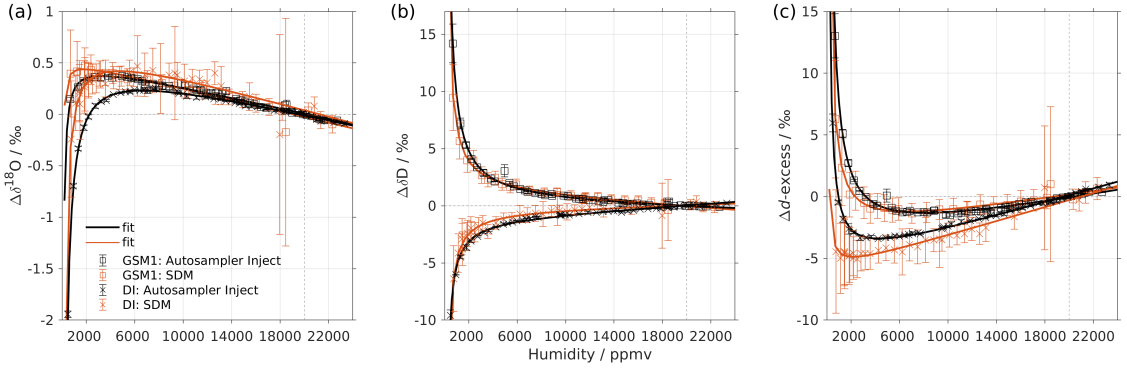

Figure 5. Humidity dependency of uncalibrated measurements from two characterisation methods for **(a)** δ^{18}O, **(b)** δD and **(c)** *d*-excess. The measurements are carried out on instrument HIDS2254 (Picarro L2130-i) with discrete injections using an autosampler (black symbols, experiment 2) or with continuous vapour streaming using a SDM (red symbols, experiment 6), both using synthetic air as the carrier gas. Symbol and error bar represents the mean and standard deviation of the last three of four injections for the measurement via the autosampler and the mean and standard deviation of the last 2–5 min of a 20–30 min long sequence for the measurement via the SDM. Solid line represents the fit using the same function as in Fig. 1. The measurements and fits for *d*-excess are calculated in the same way as in Fig. 1.

https://doi.org/10.5194/amt-2019-316
Preprint. Discussion started: 23 October 2019

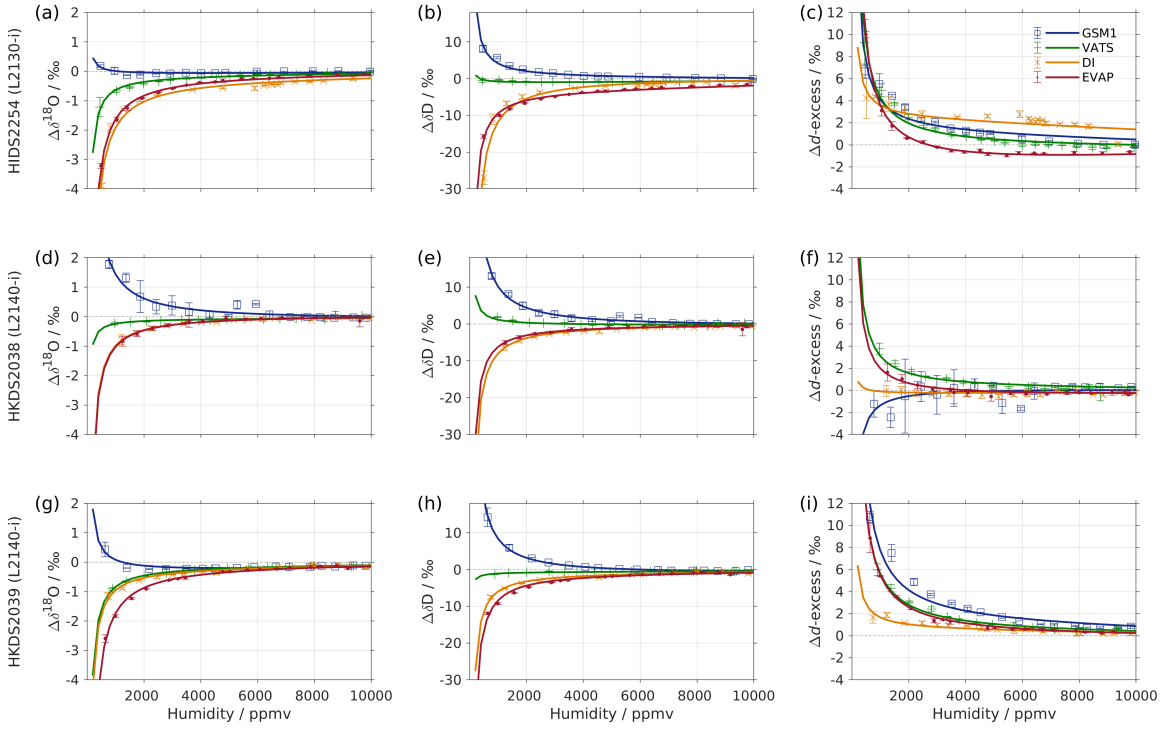

Figure 6. Humidity dependency of uncalibrated measurements for instruments **(a)–(c)** HIDS2254; **(d)–(f)** HKDS2038 and **(g)–(i)** HKDS2039. The measurements are carried out with discrete injections using an autosampler with N_2 being the carrier gas (experiment 3, 9 and 13). Only the data below 10'000 ppmv are shown. Symbols and solid lines are the same as in Fig.1.

https://doi.org/10.5194/amt-2019-316
Preprint. Discussion started: 23 October 2019

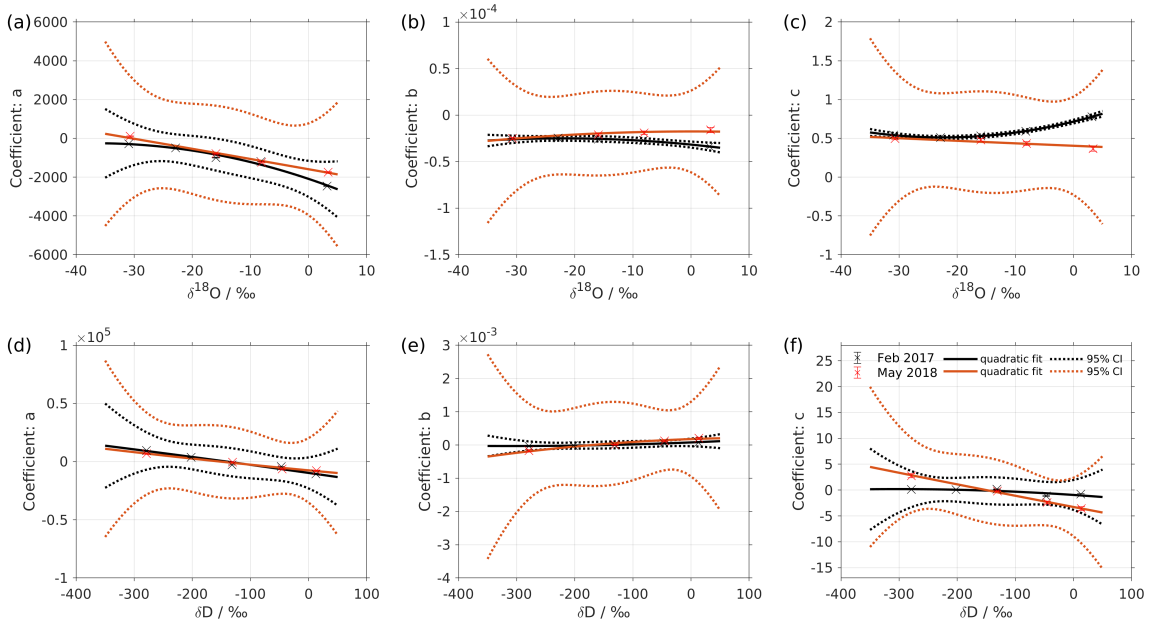

Figure 7. Same as Fig. 2, but a comparison between results in Feb 2017 (black symbols, experiment 1) and May 2018 (red symbols, experiment 2). A larger 95 % confidence interval for the fit of May 2018 (red dotted line) is due to the fewer available data points (only four standards measured).

https://doi.org/10.5194/amt-2019-316
Preprint. Discussion started: 23 October 2019

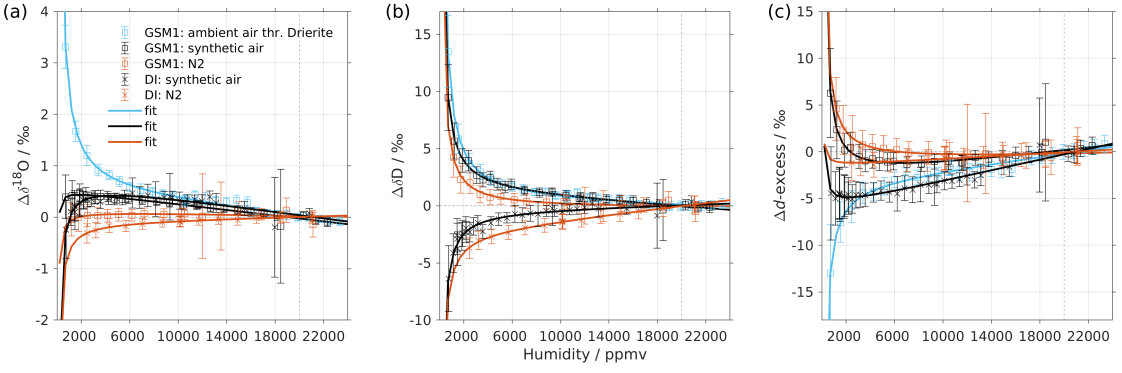

Figure 8. Same as Fig 5, but comparing between different carrier gases. The measurements are carried out on instrument HIDS2254 (Picarro L2130-i) with continuous vapour streaming via SDM (experiment 6–8). Two standard waters (GSM1 and DI) are tested with synthetic air (black symbol) and N_2 (orange symbol). The standard water GSM1 is also tested with ambient air that is dried through Drierite (blue symbol).

https://doi.org/10.5194/amt-2019-316
Preprint. Discussion started: 23 October 2019

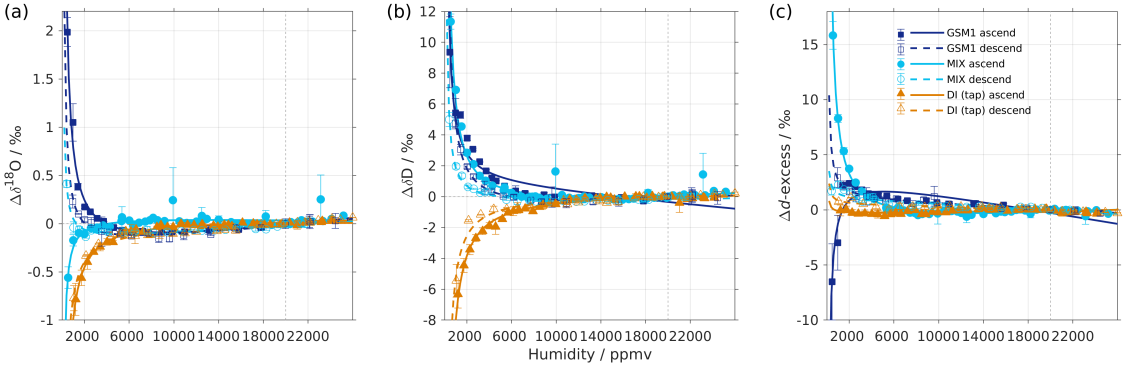

Figure 9. Humidity dependency of GSM1 (dark blue symbol), MIX (light blue symbol) and DI tap water (orange symbol) for **(a)** δ^{18}O, **(b)** δD and **(c)** *d*-excess, with ascending (closed symbol) and descending (open symbol) humidity sequences. Solid curves represent the fits for ascending humidity sequences and dashed curves the fits for descending humidity sequences. All the measurements are uncalibrated and carried out with discrete injections using an autosampler with N_2 being the carrier gas. The measurements for MIX and DI tap water are carried out on instrument HKDS2038 (Picarro L2140-i) (experiment 9). The measurements for GSM1 are carried out on instrument HKDS2039 (Picarro L2140-i) and one outlier around 500 ppmv has been excluded (experiment 14).

https://doi.org/10.5194/amt-2019-316
Preprint. Discussion started: 23 October 2019

Atmospheric Measurement Techniques Discussions

Table 1. Isotope compositions of the standard waters used in this study. The values are reported on the VSMOW2-SLAP2 scale. *FARLAB standards* are the laboratory standards in use at FARLAB, University of Bergen and *UI standards* are the laboratory standards in use at the Isotope Laboratory of University of Iceland. All the waters are laboratory working standards except MIX and DI (tap). MIX is obtained from an even mixing of GSM1 and VATS. DI (tap) is deionized tap water in Bergen, Norway. The isotope compositions of these two waters are calibrated in experiment 9 using the measured working standards. σ for *FARLAB standards* represents the standard deviation of means from six liquid injections, while σ for *UI standards* a long term standard deviation.

	δ^{18}O [‰]	σ [‰]	δD [‰]	σ [‰]	*d*-excess [‰]	σ [‰]
FARLAB standards						
GSM1	-33.07	± 0.02	-262.95	± 0.04	1.63	± 0.17
MIX	-24.78	± 0.02	-193.90	± 0.08	4.30	± 0.20
VATS	-16.47	± 0.02	-127.88	± 0.09	3.89	± 0.18
DI	-7.78	± 0.01	-50.38	± 0.02	11.83	± 0.10
DI (tap)	-7.98	± 0.01	-52.89	± 0.05	10.97	± 0.13
EVAP	5.03	± 0.02	4.75	± 0.11	-35.47	± 0.16
UI standards						
NEEM	-33.52	± 0.05	-257.11	± 0.6	11.05	± 0.72
GV	-8.54	± 0.05	-57.72	± 0.6	10.60	± 0.72
BERM	0.52	± 0.05	6.26	± 0.6	2.10	± 0.72

https://doi.org/10.5194/amt-2019-316
Preprint. Discussion started: 23 October 2019

Atmospheric Measurement Techniques Discussions

Table 2. Overview of all 14 characterisation experiments regarding the instrument, the vapour generation method, the type of dry gas supply, the measured standard waters, the humidity steps, the humidity span and the experiment time. For characterisations with injections, typically four injections are carried out at each humidity level. For characterisation with continuous vapour streaming via SDM, normally 20-40 min of measurement is carried out at each humidity level. The values of the water concentrations are the uncalibrated values measured on the corresponding analyser. Instrument HIDS2254 is model type L2130-i, while instruments HKDS2038 and HKDS2039 are of model type L2140-i.

No.	Instrument	Method	Dry gas	Standard water	Steps	Span [ppmv]	Time
1	HIDS2254	autosampler	synthetic air	GSM1, MIX, VATS, DI, EVAP	47–49	∼500–23000	Feb 2017
2		autosampler	synthetic air	GSM1, VATS, DI, EVAP	27–30	∼1000–23000	May 2018
3		autosampler	N_2	GSM1, VATS, DI, EVAP	25–29	∼500–23000	May 2018
4		SDM	synthetic air	DI	24	∼700–23000	Jul 2016
5		SDM	synthetic air	DI	11	∼1300–20000	Feb 2018
6		SDM	synthetic air	GSM1, DI	23,27	∼700–23000	Jun 2018
7		SDM	N_2	GSM1, DI	13,16	∼1200–23000	Jun 2018
8		SDM	air thr. Drierite	GSM1	27	∼700–23000	Dec 2016
9	HKDS2038	autosampler	N_2	GSM1, MIX, VATS, DI (tap), EVAP	42–44	∼800–27000	Jan 2017
10		autosampler	N_2	GSM1, VATS, DI	36,29,19	∼600–30000	Feb 2018
11		manual injection	synthetic air	NEEM, GV, BERM	8	∼2400–24000	Feb 2018
12		manual injection	synthetic air	NEEM, GV, BERM	8	∼2600–22000	Mar 2018
13	HKDS2039	autosampler	N_2	GSM1, MIX, VATS, DI, EVAP	45–47	∼500–27000	Jan 2017
14		autosampler	N_2	GSM1	20	∼500–24000	Jul 2019

https://doi.org/10.5194/amt-2019-316
Preprint. Discussion started: 23 October 2019

Atmospheric Measurement Techniques Discussions

Table 3. Summary of experiment design, ordered by the aims including the dependence on vapour generating method, the dependence on the tested instrument, the long term stability of the dependence behaviour, the influence from dry gas supply and the influence from the measuring sequence.

Experiments	Aim	Parameters tested	Conditions	Figure
2, 6	dependence on method	autosampler vs SDM	HIDS2254, synthetic air	5
3, 7	dependence on method	autosampler vs SDM	HIDS2254, N_2	not shown
3, 9, 13	dependence on instrument	three analysers	autosampler, N_2	6
1, 2	long term stability	before vs after 15 months	HIDS2254, autosampler, synthetic air	7
4, 5, 6	long term stability	before vs after 20/25 months	HIDS2254, SDM, synthetic air	not shown
9, 10	long term stability	before vs after 11 months	HKDS2038, autosampler, N_2	not shown
11, 12	long term stability	before vs after one month	HKDS2038, manual inj., synthetic air	not shown
6, 7, 8	influence from dry gas supply	synthetic air vs N_2 vs Drierite	HIDS2254, SDM	8
2, 3	influence from dry gas supply	synthetic air vs N_2	HIDS2254, autosampler	not shown
9, 14	influence from measuring sequence	ascending vs descending humidity	autosampler, N_2	not shown

https://doi.org/10.5194/amt-2019-316
Preprint. Discussion started: 23 October 2019

Atmospheric Measurement Techniques Discussions

Table 4. Fitting coefficients for the humidity dependency behaviour of the five standard waters measured on HIDS2254. Coefficients a, b, c are with respect to fitting function $f_i(x) = \frac{a_i}{x} + b_i \cdot x + c_i$. The fitting lines are shown in Fig. 1.

	Standard	a	b	c
δ^{18}O	GSM1	-274.95 ± 16.62	-2.60×10^{-5} ± 6.23×10^{-7}	0.54 ± 0.01
	MIX	-488.93 ± 9.36	-2.47×10^{-5} ± 4.73×10^{-7}	0.51 ± 0.01
	VATS	-996.35 ± 14.46	-2.59×10^{-5} ± 4.19×10^{-7}	0.53 ± 0.01
	DI	-1195.79 ± 6.53	-2.71×10^{-5} ± 3.28×10^{-7}	0.59 ± 0.01
	EVAP	-2465.30 ± 20.33	-3.39×10^{-5} ± 7.95×10^{-7}	0.78 ± 0.01
δD	GSM1	9511.99 ± 163.45	-2.96×10^{-5} ± 6.13×10^{-6}	0.12 ± 0.10
	MIX	3663.09 ± 85.40	-1.47×10^{-5} ± 4.32×10^{-6}	0.07 ± 0.07
	VATS	-2778.43 ± 64.83	-6.71×10^{-7} ± 1.88×10^{-6}	0.17 ± 0.03
	DI	-4219.07 ± 73.51	6.93×10^{-5} ± 3.69×10^{-6}	-1.15 ± 0.06
	EVAP	-10648.36 ± 168.65	7.23×10^{-5} ± 6.59×10^{-6}	-0.79 ± 0.11

https://doi.org/10.5194/amt-2019-316
Preprint. Discussion started: 23 October 2019

Atmospheric Measurement Techniques Discussions

Table 5. Fitting coefficients for the isotope composition dependency of the humidity dependency coefficients a, b and c in Table 4. Coefficients m, n and k are with respect to fitting function $f_j(y) = m_j(y - n_j)^2 + k_j$. The fitting lines are shown in Fig. 2.

	Coefficient	m	n	k
δ^{18}O	a	-1.38 $\pm$ 1.27	-36.54 $\pm$ 21.61	-252.80 $\pm$ 585.65
	b	-1.38$\times10^{-8}$ $\pm$ 4.41$\times10^{-9}$	-22.00 $\pm$ 3.14	-2.50$\times10^{-5}$ $\pm$ 7.20$\times10^{-7}$
	c	3.92$\times10^{-4}$ $\pm$ 1.30$\times10^{-4}$	-22.57 $\pm$ 3.42	0.52 $\pm$ 0.02
δD	a	-0.01 $\pm$ 0.25	-3228.00 $\pm$ 69350.00	1.04$\times10^{5}$ $\pm$ 2.35$\times10^{6}$
	b	1.19$\times10^{-9}$ $\pm$ 2.16$\times10^{-9}$	-300.00 $\pm$ 312.85	-3.00$\times10^{-5}$ $\pm$ 5.18$\times10^{-5}$
	c	-8.93e-06 $\pm$ 5.53$\times10^{-5}$	-364.70 $\pm$ 1460	0.23 $\pm$ 2.67